NASA Technical Memorandum

NASA TM-103515

TEST AND MODEL CORRELATION OF THE ATMOSPHERIC EMISSION PHOTOMETRIC IMAGER FIBERGLASS PEDESTAL

By H.M. Lee III and L.A. Barker

Structures and Dynamics Laboratory
Science and Engineering Directorate

October 1990

National Aeronautics and Space Administration

George C. Marshall Space Flight Center

NASA
National Aeronautics and Space Administration

Report Documentation Page

1. Report No.	2. Government Accession No.	3. Recipient's Catalog No.
NASA TM -103515		

4. Title and Subtitle

Test and Model Correlation of the Atmospheric Emission Photometric Imager Fiberglass Pedestal

5. Report Date: October 1990

6. Performing Organization Code:

7. Author(s)

H.M. Lee III and L.A. Barker

8. Performing Organization Report No.:

10. Work Unit No.:

9. Performing Organization Name and Address

George C. Marshall Space Flight Center
Marshall Space Flight Center, Alabama 35812

11. Contract or Grant No.:

13. Type of Report and Period Covered: Technical Memorandum

12. Sponsoring Agency Name and Address

National Aeronautics and Space Administration
Washington, DC 20546

14. Sponsoring Agency Code:

15. Supplementary Notes

Prepared by Structures and Dynamics Laboratory, Science and Engineering Directorate.

16. Abstract

This report presents the correlation of the static loads testing and finite element modeling for the fiberglass pedestal used on the Atmospheric Emission Photometric Imaging (AEPI) experiment. This payload is to be launched in the space shuttle as part of the ATLAS-1 experiment. Strain gauge data from rosettes around the highly loaded base are compared to the same load case run for the Spacelab 1 testing done in 1981. Correlation of the model and test data was accomplished through comparison of the composite stress invariant utilizing the expected flight loads for the ATLAS-1 mission. Where appropriate, the Tsai-Wu failure criteria was utilized in the development of the key margins of safety. Margins of safety are all positive for the pedestal and are reported.

17. Key Words (Suggested by Author(s))	18. Distribution Statement
Fiberglass Stress Invariant Strain Gauge	Unclassified – Unlimited

19. Security Classif. (of this report)	20. Security Classif. (of this page)	21. No. of pages	22. Price
Unclassified	Unclassified	63	NTIS

TABLE OF CONTENTS

LIST OF ILLUSTRATIONS

LIST OF ILLUSTRATIONS (Continued)

LIST OF TABLES

TECHNICAL MEMORANDUM

TEST AND MODEL CORRELATION OF THE ATMOSPHERIC EMISSION PHOTOMETRIC IMAGER FIBERGLASS PEDESTAL

INTRODUCTION

The Atmospheric Emission Photometric Imaging (AEPI) experiment pedestal was built in 1981 using F-161/1581 glass cloth, autoclave cured as 1/8-inch laminates, and meeting the specifications of MIL-P-25421. An engineering vibration test was run at that time and the pedestal was found to be too flexible (i.e., first resonant mode too low). The stiffness of the structure was increased by the bonding of additional fiberglass panels and stiffeners. It was then subjected to a vibration qualification test, and the resonant frequency was still below the required minimum of 35 Hz. The decision was made to perform a static loads test on the pedestal to 120 percent of the Spacelab 1 design loads. A later loads revision reduced this test to 113 percent of design loads. The pedestal was subsequently declared structurally qualified and was successfully flown on the Spacelab 1 mission. After the flight, inspection of the high stress regions on the pedestal revealed no visible structural defects.

In preparation for the Earth Observation Mission (EOM), minor modifications were made on some of the components mounted to the pedestal. The pedestal was vibration tested again to qualify those changes. The EOM mission was never flown, however, because of the Challenger accident.

During the post-Challenger period, the pedestal loads were altered significantly due to changes in the orbiter frequencies and forcing functions. In the process of evaluating the effects of these new loads, concern over the requirements for nonmetallic structure surfaced during an MSFC Fracture Control Board meeting in May of 1988. The decision was made to proceed with the fiberglass pedestal rather than design a new metallic one. Preliminary stress analyses had shown the design was sound.

A question was raised concerning fiberglass strength deterioration due to age. Criteria for determining time-related deterioration were nonexistent. Attempts were made to develop such criteria by consulting the Materials and Processing Laboratory at MSFC and some fiberglass experts at the Langley Research Center (LaRC). To prove the current integrity of the fiberglass strength, tensile samples were cut from a spare fiberglass part built at the same time and by the same process as the flight hardware. The fiber orientation of these samples was random (as compared to the 0, 90, and ± 45 layups for the pedestal). The angle of each layer was determined through delamination procedures after the testing. Test results showed good agreement with strength tests from the pedestal when it was originally built. Appendix A gives the comparison of these data. The conclusion is that strength degradation, due to age, is negligible. Additionally, photographs of highly-loaded areas were taken in both visible and ultraviolet light. These photos showed halos of lighter color around most attachment structures where steel fasteners were used, and revealed some possible "defects" in several other areas. The photos were supplied to personnel at LaRC. They suggested that MSFC might accomplish dye penetrant testing for possible debonding. This approach

was later discarded because no criteria existed to measure the speed of the wicking to determine if damage had occurred, and the dye would present an outgassing problem in space. Although no obvious damage was apparent, the extent of undetectable damage due to its previous flight, testing, and handling was still unknown. The pedestal was classified as a fracture-critical component [1].

For the above reasons, and because previous finite element models had not correlated well with test data, it was decided to develop a completely new analytical model and perform a static loads test to 120 percent of the new ATLAS-1 mission loads. The testing would be accomplished by the MSFC Structural Test Division.

DERIVATION OF TEST LOADS

The AEPI fiberglass pedestal (fig. 1) is considered fracture-critical hardware. In addition, numerous "indications" are present on the surface and have been photographically documented. For this reason and the fact that nondestructive evaluation (NDE) is so subjective for this material, it was decided to statically load test the flight unit to 1.2 times the worst case ATLAS-1 flight loads. To calculate test loads, the component weights and centers of gravity (table 1) and the ATLAS-1 load factors (table 2) are required. The actual test setup had only three fixtures at which load could be introduced: the detector/cradle (C), the pointing mount/gimbal (B), and the mount electronics (A). This left the pedestal/cable weight (125 lb) and the aperture door (6.6 lb) to be accounted for. The procedure used to calculate the actual test forces at each fixture was as follows:

1. Single axis random in the X-axis was found to always be the worst case for the pedestal $(Q_x + R_x, Q_y, Q_z)$.

2. Worst case pedestal stresses were generated from four load combinations of $(Q_x + R_x, Q_y, Q_z)$: $(+++)$, $(++-)$, $(+-+)$, and $(+--)$.

3. The maximum stresses produced by the four cases were tension for some locations and compression for others. The four remaining cases $(---)$, $(--+)$, $(-+-)$, and $(-++)$ were added to the test sequence to assure that maximum tension and maximum compression would be exercised on both sides of the pedestal base.

4. The forces and moments effectively being transferred to the base of the pedestal were determined for 1.2 times ATLAS-1 flight loads.

5. The common load factor (LF) necessary to obtain the same moments at the pedestal base for the test condition (LF $\times$ (ATLAS-1 loads)) using only the three given test fixtures was determined.

Table 3 shows a comparison of the pedestal base forces and moments for the ATLAS-1 flight loads times 1.2 versus these derived test loads. Only cases 2 through 5 are shown; however, cases 6 through 9 are the same in magnitude but opposite in sign. In no case was the LF greater than 1.45. This meant that in the local region of each test fixture, the loading was ≤ 1.45 times ATLAS-1 flight loads. Stress analysis of these loading conditions was accomplished to make sure that the fiberglass hardware never saw >80 percent of its ultimate strength during testing. It should

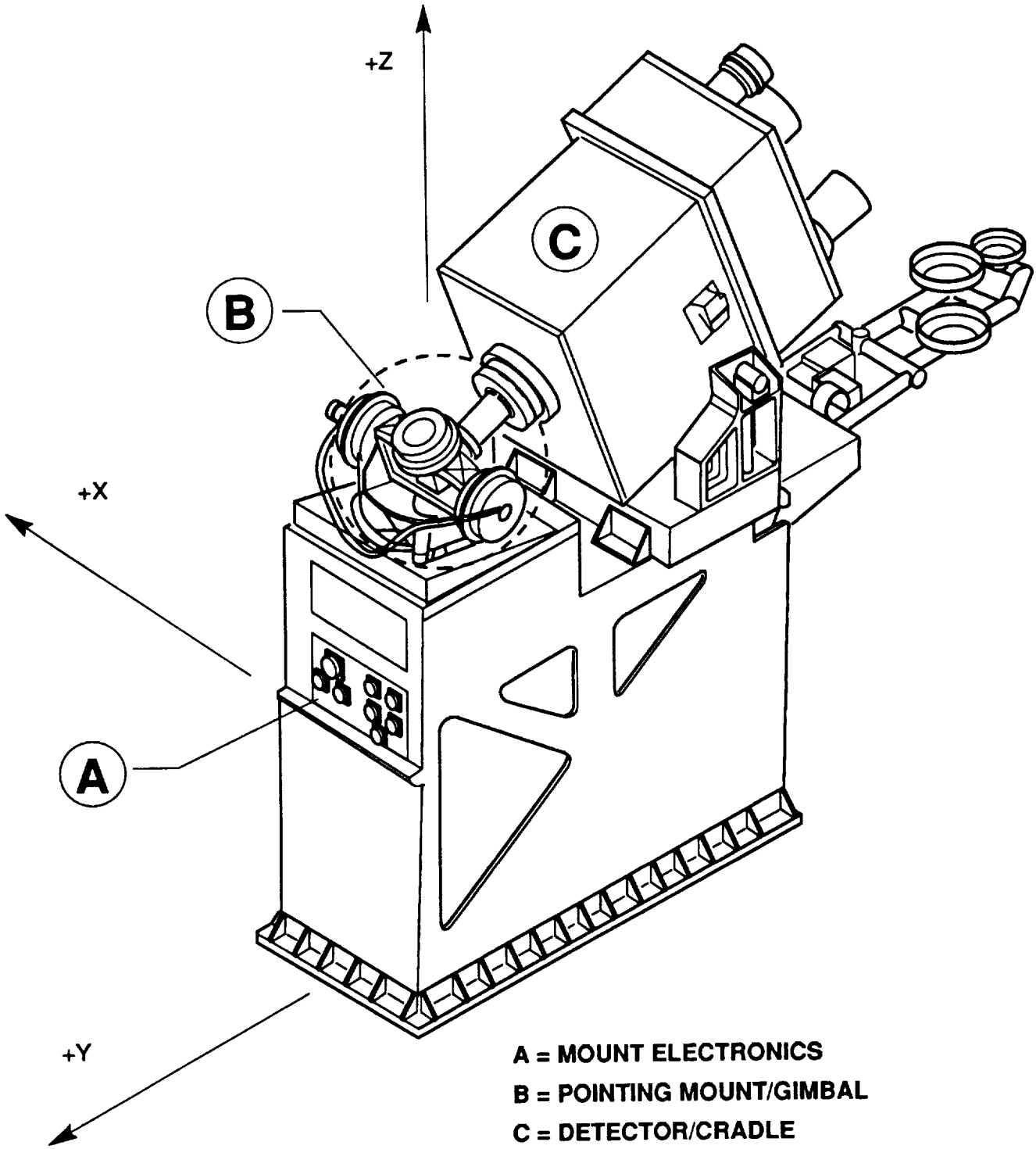

Figure 1. AEPI fiberglass pedestal.

Table 1. AEPI weights and centroids.

Description	Weight (lb)	X (in)	Y (in)	Z (in)
Detector Assembly	127.21	1,089.90	-37.80	438.48
Pointing Mount	33.07	1,089.90	-12.10	437.00
Pedestal+Cable+MLI	124.91	1,089.90	-24.90	412.53
Mount Electronics	37.48	1,089.90	-15.94	421.54
Cradle/Locks	25.57	1,089.90	-35.20	429.30
Aperture Door	6.61	1,089.90	-58.00	432.30
Bumper Rail	13.89	1,089.90	-8.80	436.50
Total	368.74			

Table 2. AEPI load factors.

From Memo P321 (ATLAS-1) 88-024

Liftoff Accelerations

Description	XMAX	XMIN	Y	Z
Detector Assembly	+6.7	-10.0	+/-2.5	+/-2.8
Pointing Mount	+3.0	-6.4	+/-2.5	+/-2.8
Aperture Door	+2.8	-6.3	+/-2.4	+/-3.1
Mount Electronics	+2.0	-5.6	+/-2.2	+/-2.8
Pedestal	+2.2	-5.8	+/-2.2	+/-3.0

Landing Accelerations

Description	X	Y	ZMAX	ZMIN
Detector Assembly	+/-9.9	+/-4.0	+5.1	-2.2
Pointing Mount	+/-6.7	+/-3.8	+5.3	-1.5
Aperture Door	+/-7.3	+/-3.7	+6.0	-3.0
Mount Electronics	+/-5.7	+/-3.3	+5.2	-1.5
Pedestal	+/-6.1	+/-3.2	+5.7	-2.7

From Memo ED23-88-139

Random Accelerations	X	Y	Z
	+/-3.6	+/-2.7	+/-5.1

be noted here that case 1 was 50 percent of an SL-1 load case that had been tested in 1981 and for which data were still available. This case was used to check out the load cells and the instrumentation. In addition, it provided a good data point to determine if the basic pedestal stiffness had changed [2].

Tables 4 and 5 tabulate the actual test loads utilized at the three load fixtures for cases 1 through 5 and cases 6 through 9, respectively.

TEST INSTRUMENTATION

The entire test setup, including installation of strain gauges, was skillfully assembled by the MSFC Structural Test Division. The test hardware consisted of the as-modified flight pedestal (MSFC drawing 42A10627), 3 load fixtures with load carrying capability at the centroid of each component (fig. 1), a Spacelab orthogrid panel for supporting the base of the pedestal, 9 hydraulic cylinders and associated load cells, 14 uniaxial strain gauges, 18 triaxial strain gauges, and 15 deflection gauges [3]. Figures 2 through 7 show the location of each strain and deflection gauge on the pedestal. Triaxial strain gauges T1001 through T1016 are the gauges primarily utilized in the correlation process. As can be seen, these gauges are located around the entire base of the pedestal where the stress state is the greatest magnitude. Deflection gauges D1001 through D1004 and D1009 reveal the X-axis motion, while gauges D1005 through D1008 show Y-axis motion. Deflection gauges D1010 through D1015 were located in the Z-axis on the aluminum base angle where it attached to the orthogrid structure. These gauges were later used to help develop an understanding of the base attach boundary condition.

SPACELAB 1 LOAD CASE COMPARISON

As mentioned previously, the pedestal had been load tested in 1981 to 113 percent of the expected Spacelab 1 flight loads. Locations of the strain and deflection gauges for the ATLAS-1 loads were the same, therefore, it was deemed prudent to repeat one of the Spacelab 1 load cases. Repeat of this load case would provide good data for determining if the structure had changed significantly with time. In addition, it would provide a reasonable check of the instrumentation and load cells.

Displacement gauges (Z-axis) located on the orthogrid shelf and associated floor attachment hardware indicated that there was significant motion during each test sequence. Six gauges (D1010 through D1015) clearly revealed that the pedestal was attached to a much more compliant structure during the 1989 testing. Table 6 shows the magnitude of the six gauges in relation to the test cases. This difference in boundary may appreciably affect the stresses on the lower pedestal near the orthogrid attach. Table 7 compares the X-axis and the Y-axis displacement gauges (D1001 through D1009) from both 1981 and 1989 tests. This table attempts to analytically remove the effects of the base motion from the displacements.

Table 3. Test loads versus 1.2 x flight loads.

CASE	LOADS AT BASE OF PEDESTAL					
	FX	FY	FZ	MX	MY	MZ
		(lb)			(in-lb)	
2 (+ + +)						
1.2 X FLIGHT LOADS	4,958	1,047	1,271	-38,909	163,835	27,424
TEST LOADS (LF=1.44)	4,164	838	956	-37,604	165,355	27,916
3 (+ + -)						
1.2 X FLIGHT LOADS	4,958	1,047	-1,271	-31,213	166,021	27,424
TEST LOADS (LF=1.45)	4,193	844	-963	-28,562	167,400	28,118
4 (+ - +)						
1.2 X FLIGHT LOADS	4,958	-1,047	1,271	31,213	163,835	25,620
TEST LOADS (LF=1.45)	4,193	-844	963	28,562	165,743	26,667
5 (+ - -)						
1.2 X FLIGHT LOADS	4,958	-1,047	-1,271	36,475	166,002	25,620
TEST LOADS (LF=1.44)	4,164	-838	-956	37,600	166,245	26,480

THESE LOADS ASSURE A 1.2 X FLIGHT LOADS AT PEDESTAL BASE (CRITICAL AREA), AND PLACE A (LF) X FLIGHT LOADS AT THE 3 TEST LOAD POINTS.

Table 4. ATLAS-1 test loads (lb) – cases 1 through 5.

LOAD POINT	AXIS	SL-1 TEST	CASE			
		1	2	3	4	5
ELECTRONICS BOX A	X	504	496	500	500	496
	Y	288	119	120	-120	-119
	Z	975	151	-152	152	-151
GIMBAL MOUNT B	X	375	676	680	680	676
	Y	213	169	170	-170	-169
	Z	726	189	-190	190	-189
DETECTOR C	X	1,701	2,992	3,013	3,013	2,992
	Y	969	550	554	-554	-550
	Z	3,292	616	-620	620	-616

CASE 1 = SL-1 LOAD TEST + + +, WILL RUN TO 50%

CASE 2 = ATLAS-1 LOAD + + +, 1.2 X AT PEDESTAL BASE, 1.44 X AT TEST LOAD POINTS

CASE 3 = ATLAS-1 LOAD + + -, 1.2 X AT PEDESTAL BASE, 1.45 X AT TEST LOAD POINTS

CASE 4 = ATLAS-1 LOAD + - +, 1.2 X AT PEDESTAL BASE, 1.45 X AT TEST LOAD POINTS

CASE 5 = ATLAS-1 LOAD + - -, 1.2 X AT PEDESTAL BASE, 1.44 X AT TEST LOAD POINTS

Table 5. ATLAS-I test loads (lb) – cases 6 through 9.

LOAD POINT	AXIS	CASE			
		6	7	8	9
ELECTRONICS BOX A	X	-496	-500	-500	-496
	Y	-119	-120	120	119
	Z	-151	152	-152	151
GIMBAL MOUNT B	X	-676	-680	-680	-676
	Y	-169	-170	170	169
	Z	-189	190	-190	189
DETECTOR C	X	-2,992	-3,013	-3,013	-2,992
	Y	-550	-554	554	550
	Z	-616	620	-620	616

CASE 6 = ATLAS-1 LOAD - - -, 1.2 X AT PEDESTAL BASE, 1.44 X AT TEST LOAD POINTS

CASE 7 = ATLAS-1 LOAD - - +, 1.2 X AT PEDESTAL BASE, 1.45 X AT TEST LOAD POINTS

CASE 8 = ATLAS-1 LOAD - + -, 1.2 X AT PEDESTAL BASE, 1.45 X AT TEST LOAD POINTS

CASE 9 = ATLAS-1 LOAD - + +, 1.2 X AT PEDESTAL BASE, 1.44 X AT TEST LOAD POINTS

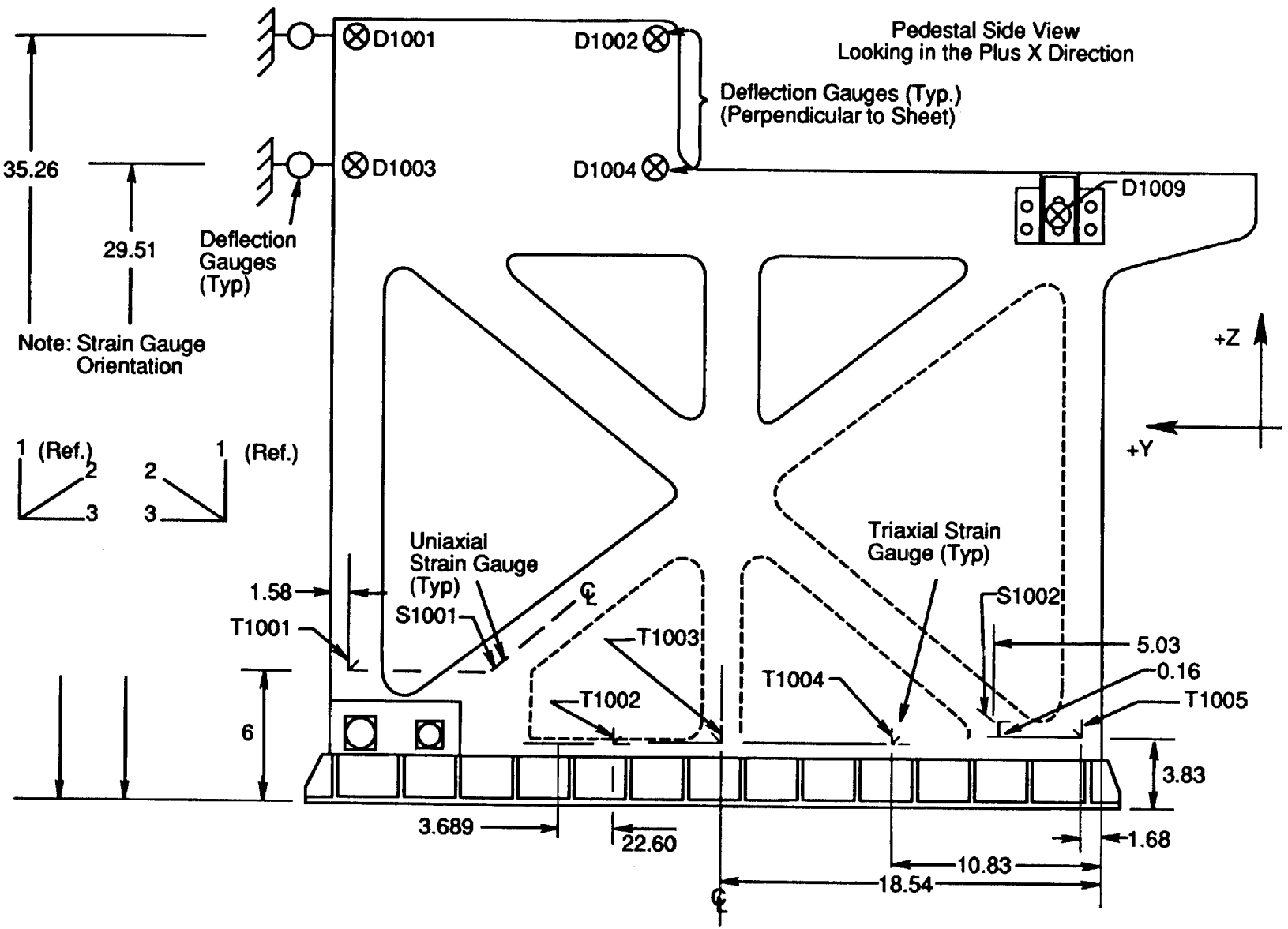

Figure 2. AEPI pedestal static structural test instrumentation requirements.

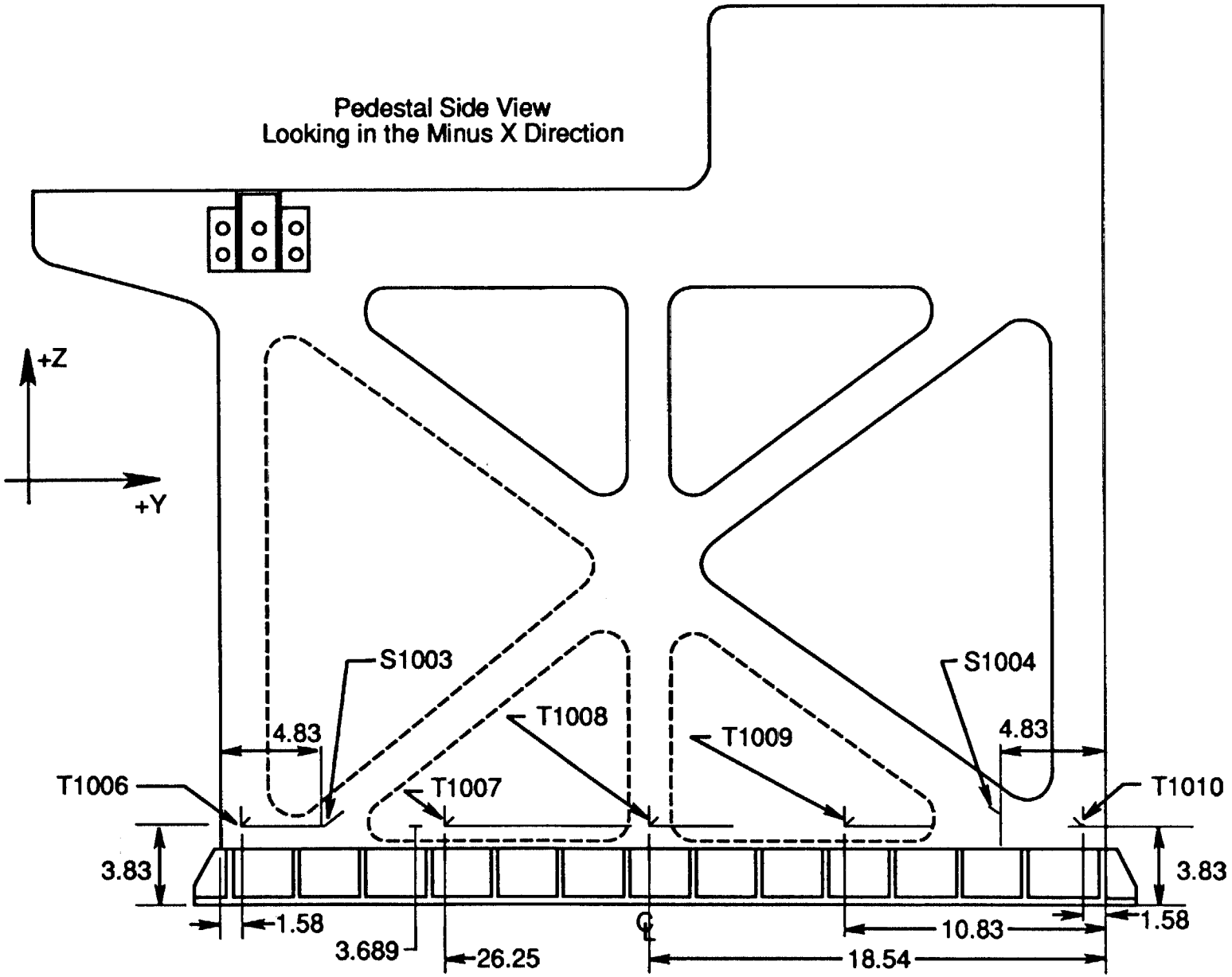

Figure 3. AEPI pedestal static structural test instrumentation requirements.

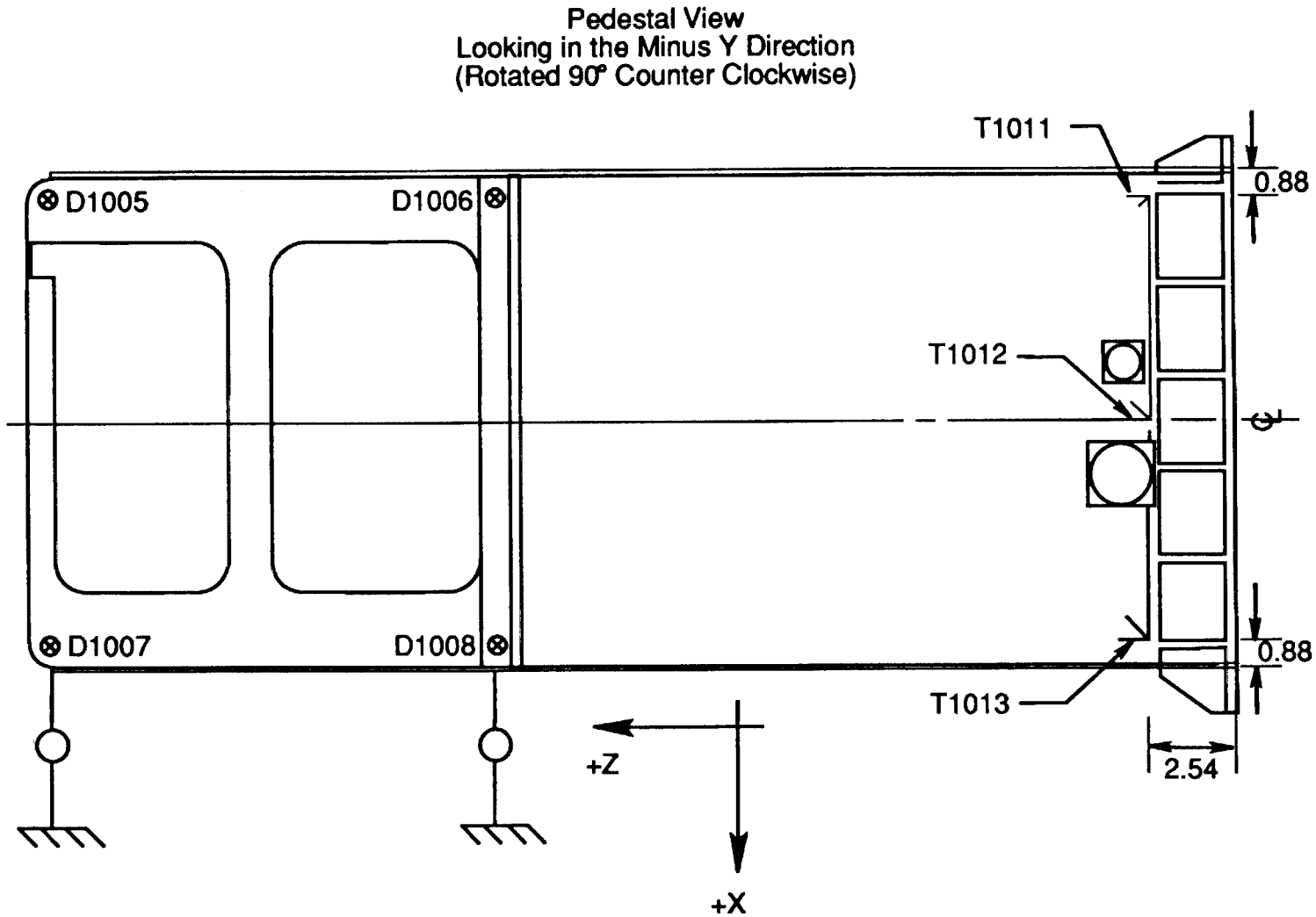

Figure 4. AEPI pedestal static structural test instrumentation requirements.

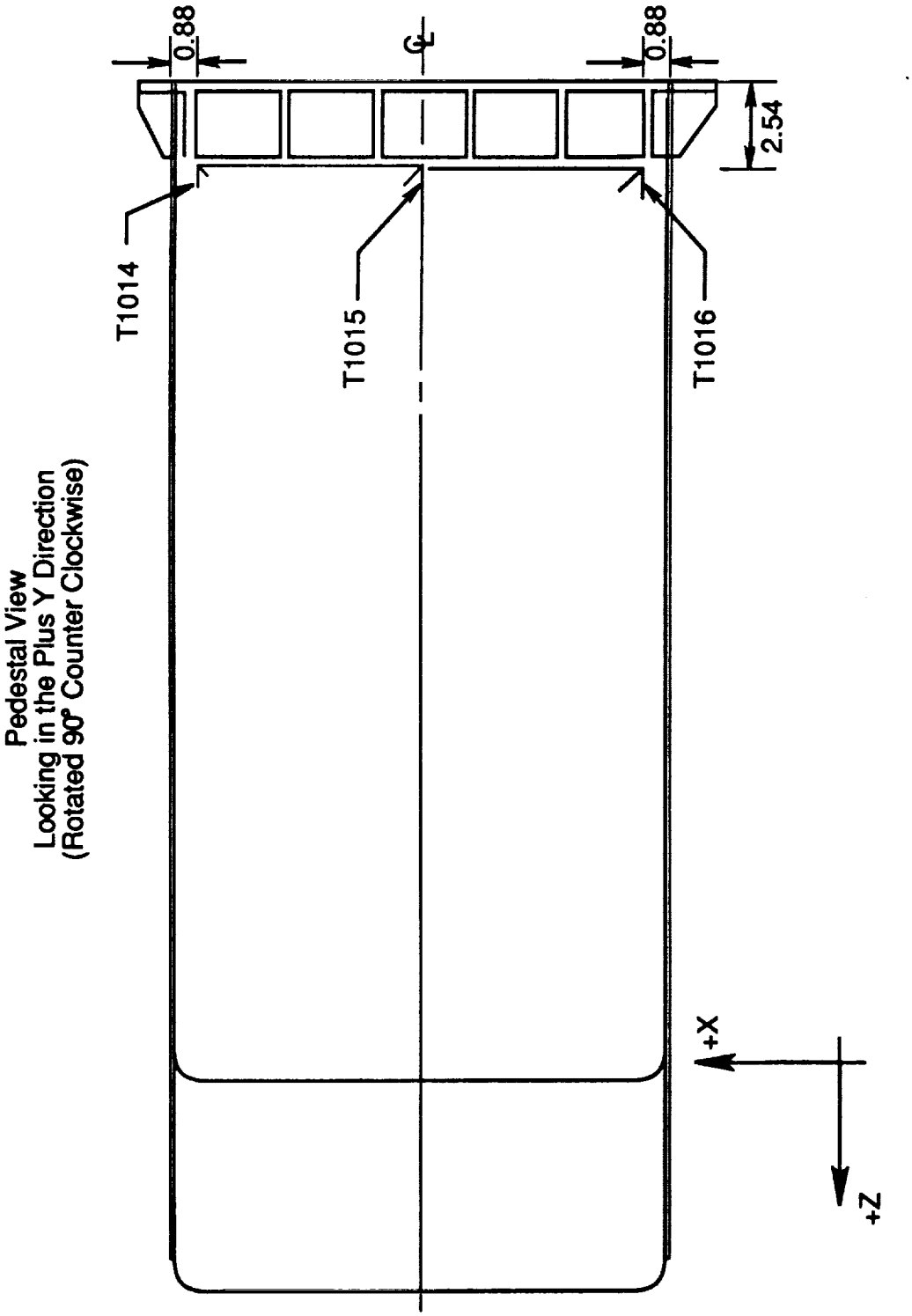

Figure 5. AEPI pedestal static structural test instrumentation requirements.

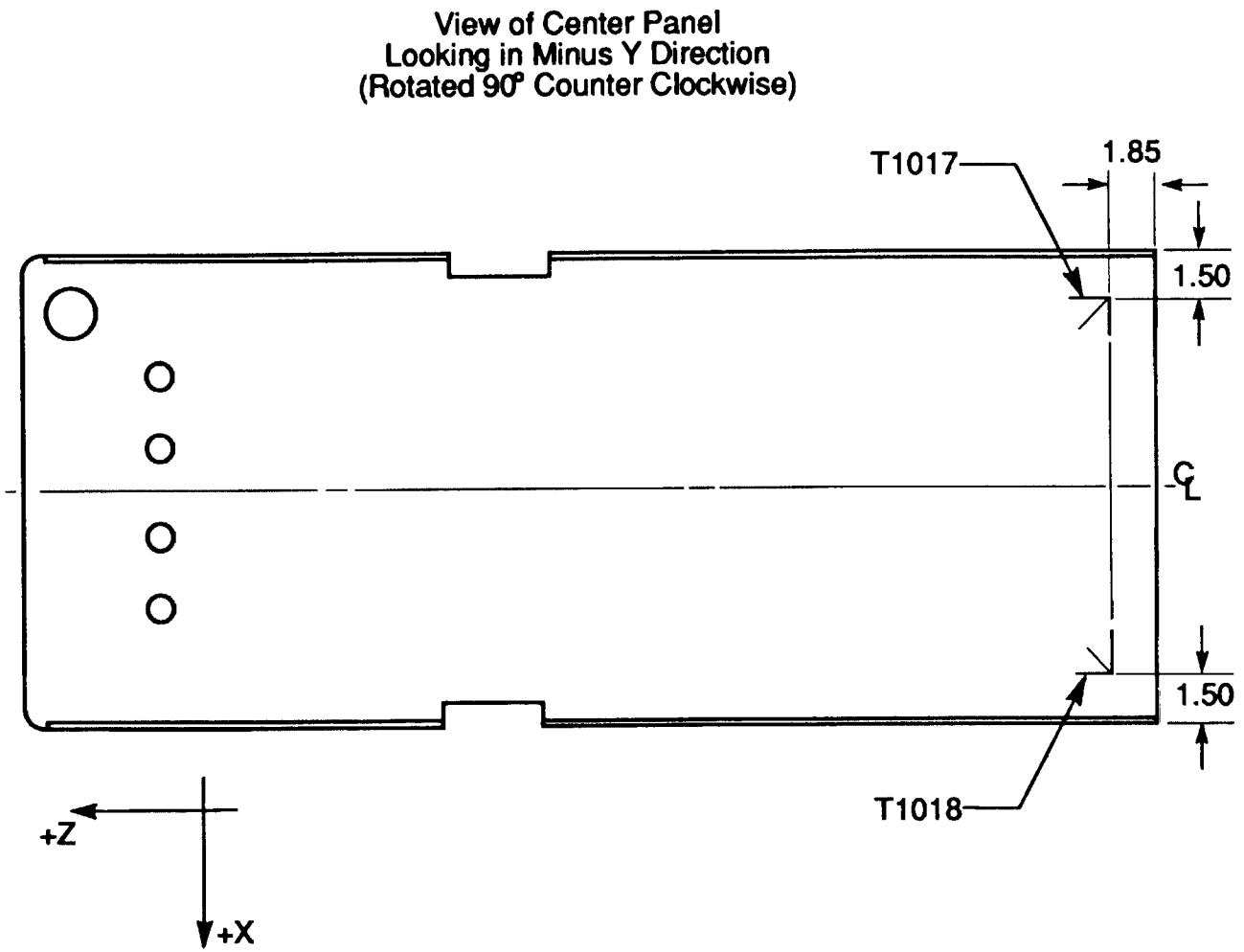

Figure 6. AEPI pedestal static structural test instrumentation requirements.

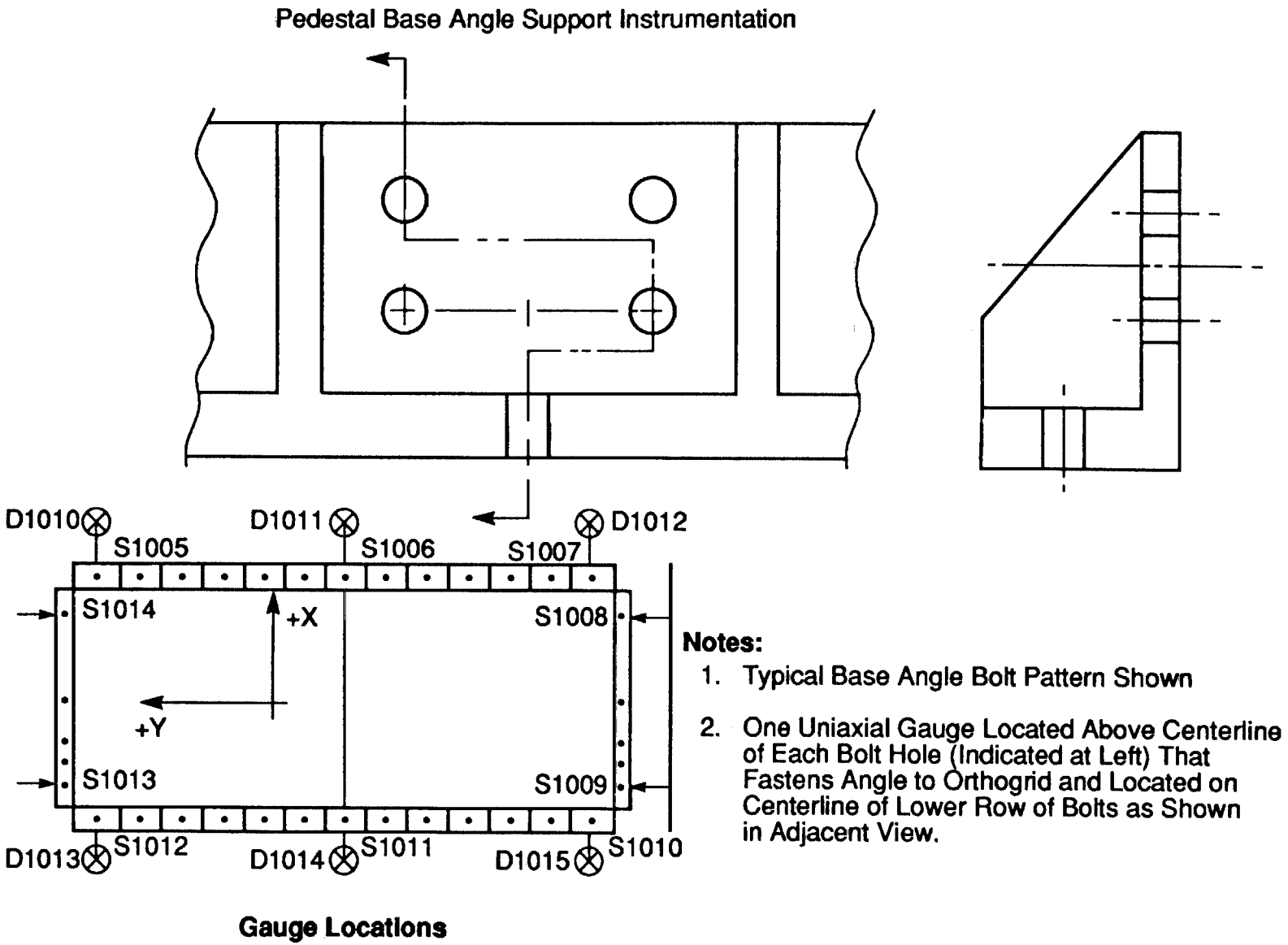

Figure 7. AEPI pedestal static structural test instrumentation requirements.

Table 6. Test fixture base motion (Z).

(INCHES)

CASE	DISPLACEMENT GAUGE D1010	D1011	D1012	D1013	D1014	D1015
1(1981)	-.001	.000	.000	+.004	+.004	+.009
1(1989)	-.004	-.002	.000	+.016	+.015	+.021
2	-.033	-.032	-030	+.043	+.048	+.054
3	-.035	-.034	-.033	+.038	+.042	+.049
4	-.028	-.032	-.034	+.041	+.042	+.046
5	-.030	-.033	-.037	+.041	+.043	+.045
6	+.040	+.038	+.041	-.033	-.038	-.039
7	+.044	+.044	+.048	-.030	-.035	-.035
8	+.037	+.037	+.045	-.036	-.039	-.030
9	+.041	+.041	+.047	-.031	-.034	-.030

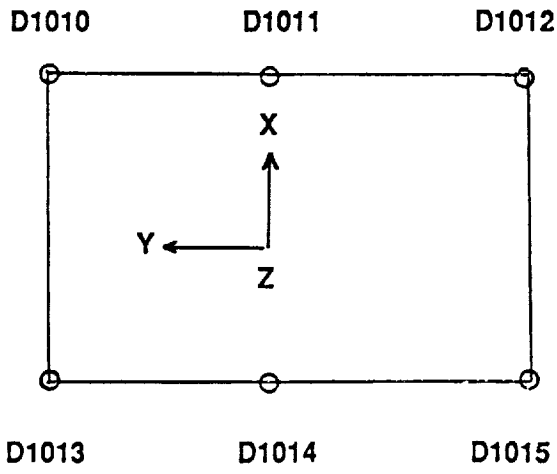

Table 7. Comparison of displacements for case 1.

SL-1 1981 TEST VS. SL-1 1989 TEST
[50% LOAD (+++)]

GAGE	SL-1 1981	SL-1 1989		AXIS
			RERUN	
D1	-.0437	-.0315	-.0377	X
D2	-.0427	-.0335	-.0377	X
D3	-.0328	-.0301*	-.0341*	X
D4	-.0348	-.0291	-.0351	X
D9	-.0275	-.0312	-.0381	X
D5	.021	.0200	.0190	Y
D6	.011	.0100	____	Y
D7	.022	.0210	.0210	Y
D8	.010	.0100	.0100	Y

ALL MEASUREMENTS IN INCHES

where:

$D_1 = D_{1001} + (D_{1013} + D_{1014} + D_{1010} + D_{1011})\ (1/2)\ (36.26/14.43)$

$D_2 = D_{1002}$ + same as above

$D_3 = D_{1013} + D_{1014} + D_{1010} + D_{1011})(1/2)(36.26-6.75)/14.43$

*D_3 appears erroneous throughout

$D_4 = D_{1004}$ + same as above

$D_9 = D_{1009} + (D_{1012} + D_{1015}/14.43)\ (36.26 - 6.75 - 1.5)$

(These calculations attempt to remove effects of base motion.)

An initial review of the resulting stresses from both 1981 and 1989 test programs revealed a very poor comparison. Further investigation of the 1981 test concluded that the strains were read from the gauges directly and fed into a computer program that calculated the maximum stress, minimum stress, shear stress, and angle of principal stress using an isotropic Mohr's circle approach. This is known today to be erroneous for composites which exhibit directional stiffness and strength characteristics. Utilizing a modulus of elasticity of $3.0 \times x10^6$ psi and a Poisson's ratio of 0.12 (fig. 8), the rosette strain gauge readings (ε_1, ε_2, ε_3) for the 1981 test were back calculated (see appendix B). Figures 9 through 11 show comparative plots of these strains around the base of the pedestal for both tests. As can be seen, both tests exhibit the same general characteristics.

The final evaluation of test data was done by plotting what is known as a stress invariant for each load case. Invariants are combinations of stress components that remain constant even under coordinate transformation. They are good indicators, for composite materials, of how each test case effectively loaded the pedestal. The invariant was calculated as follows:

$$\sigma_{inv} = (\sigma_x^2 - \sigma_x\sigma_y + \sigma_y^2 + 3\tau_{xy}^2)^{1/2}$$

where:

σ_x = tensile or compression stress in x-axis

σ_y = tensile or compression stress in y-axis

τ_{xy} = shear stress in x-y plane.

Figure 12 depicts the comparison of the invariant stress for the Spacelab 1 1981 versus the Spacelab 1 1989 test. This final figure shows good agreement between the two tests and indicates that no significant structural difference is present as a function of time.

Based on analysis of the test data, it is concluded that:

1. The ATLAS-1 testing had a much less rigid floor attachment system than did the Spacelab 1 tests. The ATLAS-1 test condition will, therefore, be more difficult to analytically simulate.

2. Deflections in the X and Y axes of the pedestal indicated, within the accuracy of the gauges, that no clearly detectable stiffness changes have occurred since the 1981 testing.

3. Examination of the rosette strain gauge readings around the pedestal base shows relatively good comparison between the 1981 and 1989 testing. Identical magnitudes for both tests were probably not possible due to the difference in floor stiffness.

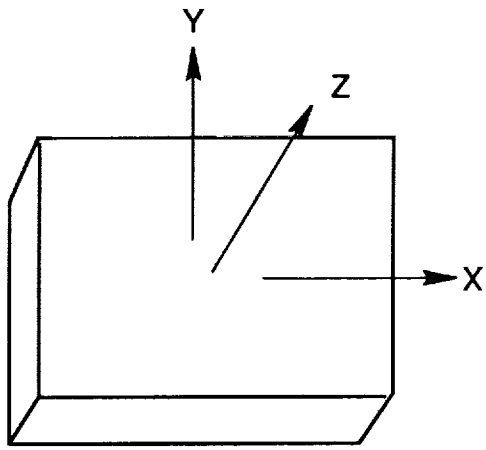

Ô **Material Properties**

E_x = 3.0 x 10^6 psi (Test)

E_y = 2.9 x 10^6 psi (Test)

E_z = 0.5 x 10^6 psi (Vendor Data)

G_{xy} = 0.45 x 10^6 psi

$G_{zx} = G_{yz}$ = 0.27 x 10^6 psi

$\nu_{xy} = \nu_{zx} = \nu_{yz}$ = 0.12 (Vendor Data)

- 1/8" Laminate
- 1581 Glass Cloth
- Autoclave Cured
- Mil-P-25421

○ **Strength**

FTU (0°) = 43.3 ksi (Tests)

FTU (45°) = 21.5 ksi (Tests)

FTU (90°) = 36.2 ksi (Tests)

FSU = 10.7 ksi (Calculated)

FBR = 28 ksi (Tests) - Bearing

FSIL = 2,100 psi (Vendor Data) - Interlaminar Shear

Figure 8. Fiberglass mechanical properties.

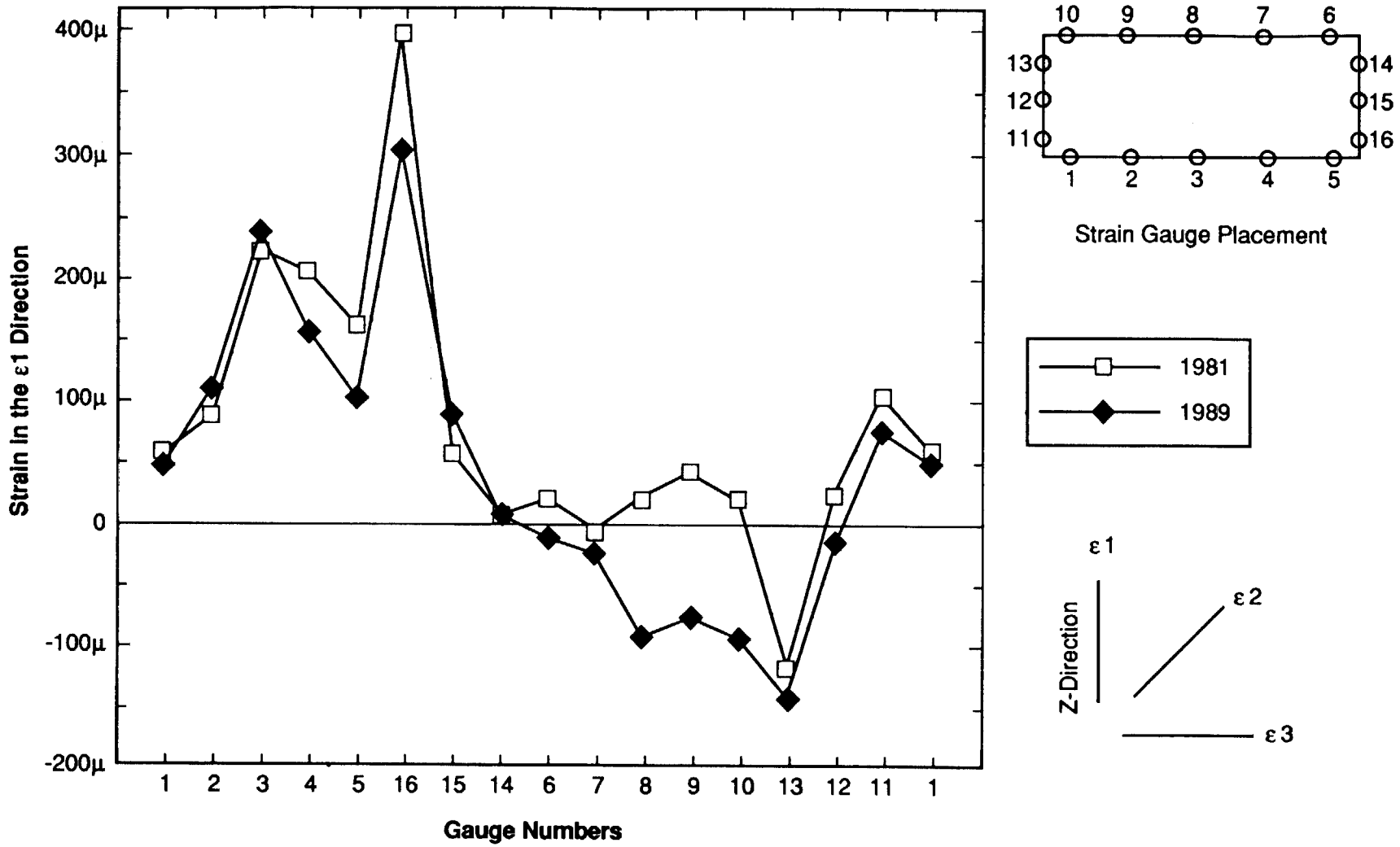

Figure 9. Comparison of strain in the ε_1 direction between 1981 and 1989 test data.

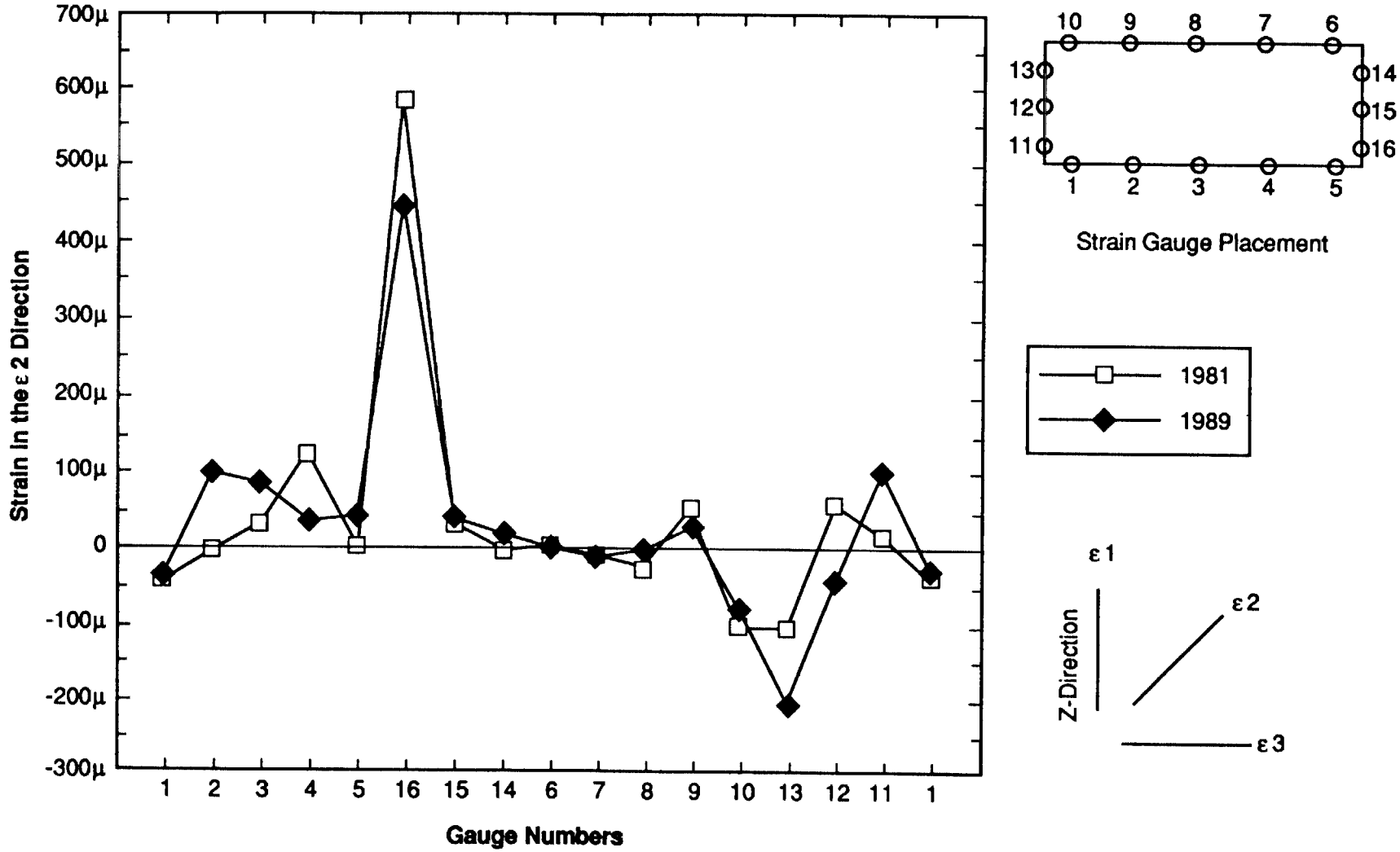

Figure 10. Comparison of strain in the ε_2 direction between 1981 and 1989 test data.

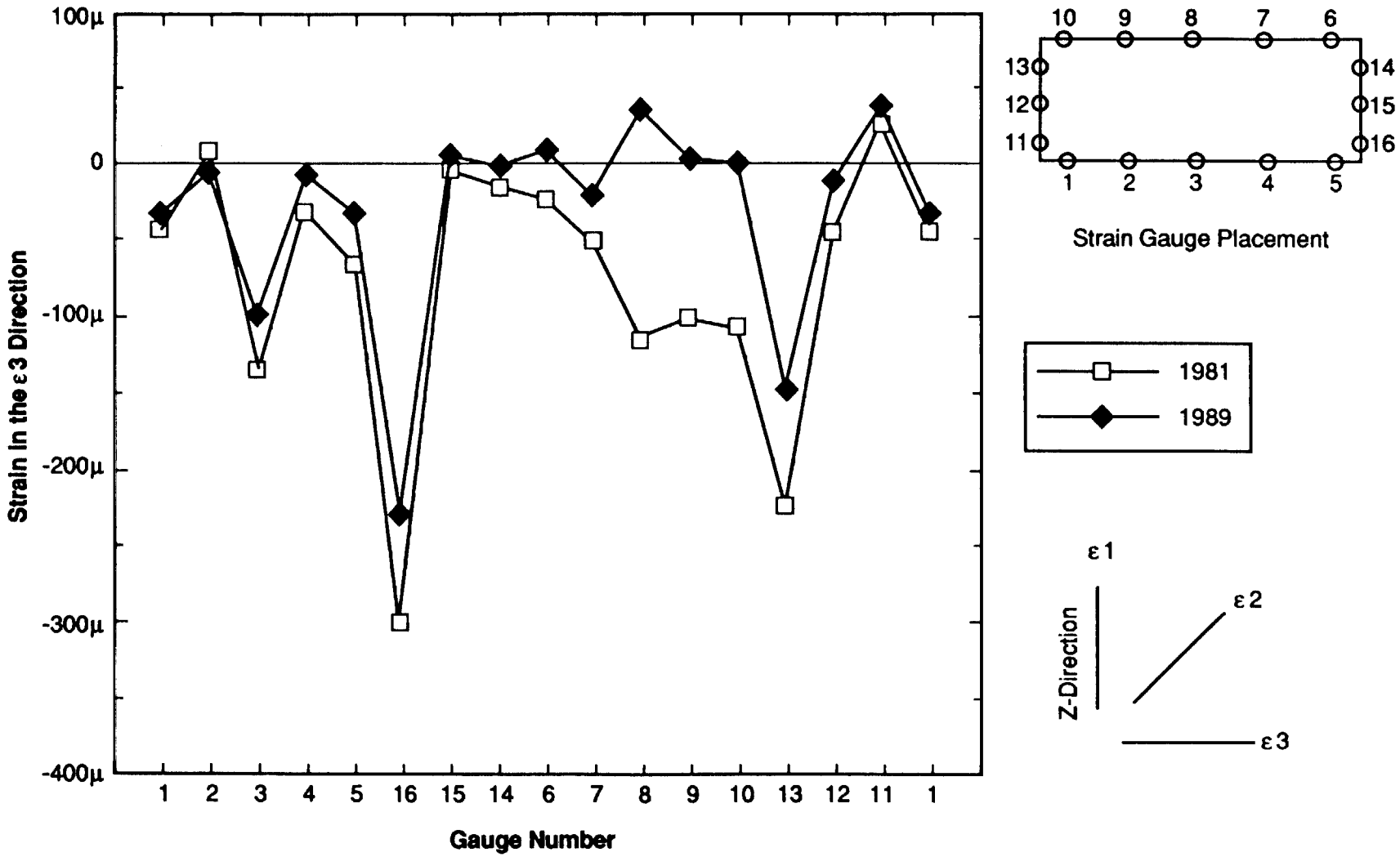

Figure 11. Comparison of strain in the ε_3 direction between 1981 and 1989 test data.

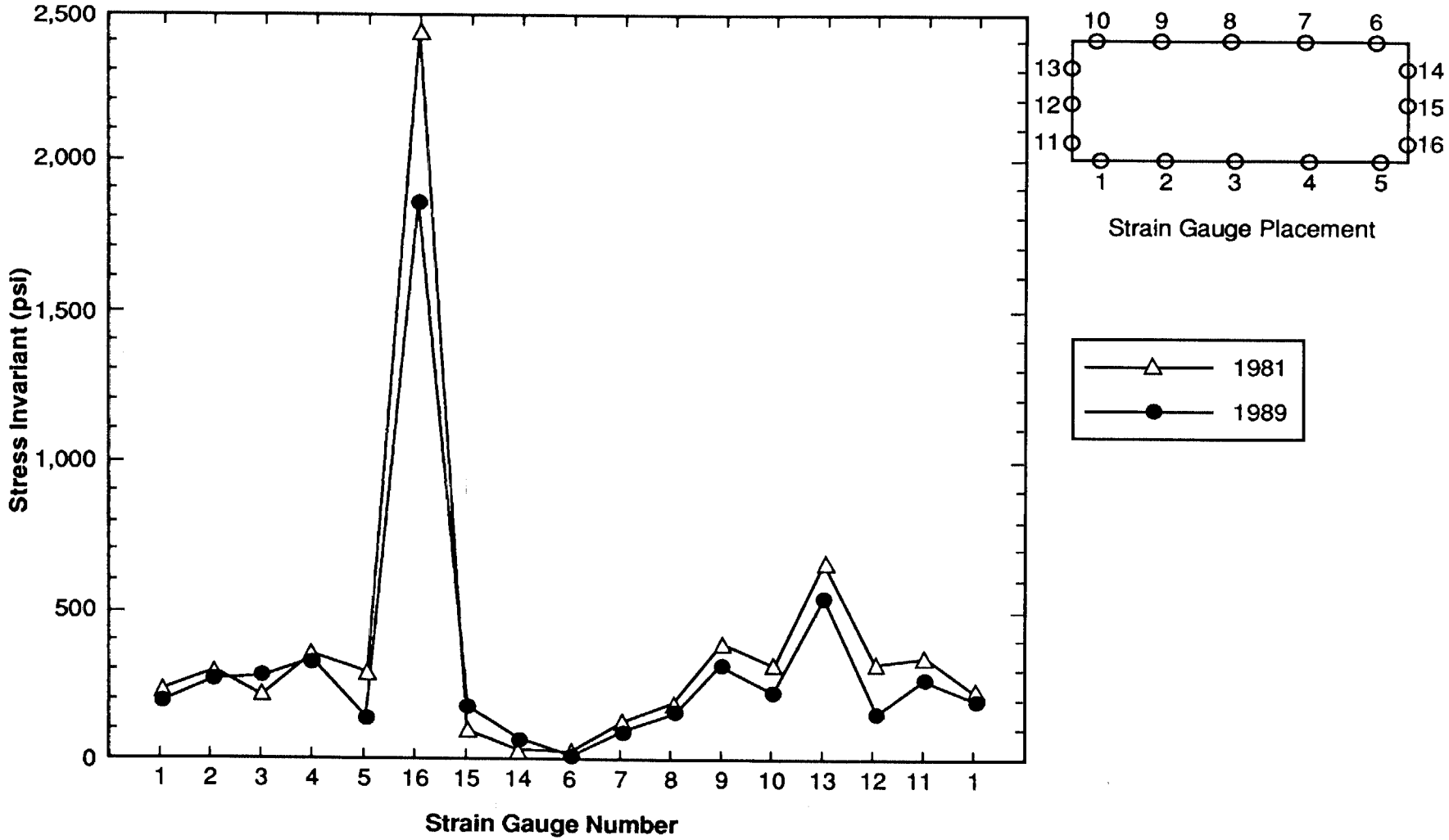

Figure 12. Comparison of stress invariants for 1981 and 1989.

MATH MODEL DESCRIPTION

A finite element model was built of the AEPI fiberglass pedestal. The ANSYS structural code was utilized in the performance of the analysis. The model consisted of 19,639 nodes and 4,259 STIF91 elements. This element is a layered version of the 8-node isoparametric shell, and up to 16 different material layers can be modeled. In this analysis, a layer consisted of fiberglass panels 0.125 inches thick. In the case of the base angle attach region, the hardware has up to five layers including the aluminum angle. Initially the base of the pedestal (where it attaches to the orthogrid panel) was assumed to be fixed. It soon became apparent that the attachment fixturing used in test, including the orthogrid, was far from stationary. The previously mentioned base motion was simulated by enforcing test measured displacement (Z) around the entire base of the pedestal. The detector, gimbal assembly, and the electronics box were modeled as relatively rigid structures, attaching at the proper locations on the pedestal. For test simulations, loads were applied directly to these rigid test fixtures. For flight conditions, the loads were again applied by forces at the rigid component structures, while the pedestal loads were applied by accelerations. Plots of the undeformed model can be seen in figures 13 through 18.

TEST/MODEL CORRELATION

The finite element model was built primarily to validate the hand analysis. To make sure that the model would properly predict margins of safety for flight loads, it needed to be test verified. The loads applied to the model are the same eight loading cases (cases 2 through 9) applied during the testing. An attempt was made to simulate the boundary conditions that were present on the pedestal. The actual applied loads caused the orthogrid structure to move much more than was anticipated. The six deflection gauges mounted on the base angle were used to measure this motion. To replicate this in the model, deflections were assumed to be linear between gauges. The six measured displacements were used to calculate enforced displacements on the model for all eight load cases.

All of the material properties required to execute the model were not known for the fiberglass (fig. 8). The in-plane shear modulus (Gxy) for the laminate was the most critical property in this category. The known properties were taken from either in-house test results or were from vendor-supplied data. These known properties were input to the model and then the deflection data were used to tune the material modulus so that the model displacements matched the test deflection gauge data.

The displacements from the test and model were then compared directly for gauges D1 through D4 and D9. Gauges D5 through D8 were not compared because they were in the noise floor of the gauges. Gauge D3 consistently read a higher displacement than was thought to be possible, and the model results agreed with this conclusion. It has been assumed that gauge D3 is erroneous throughout the testing (figs. 19 through 22). For the stress comparison, the stress invariant was again calculated at each strain gauge location. As noted previously, the invariant gives a measure of the stress independent of coordinate orientation. To compare the model and test

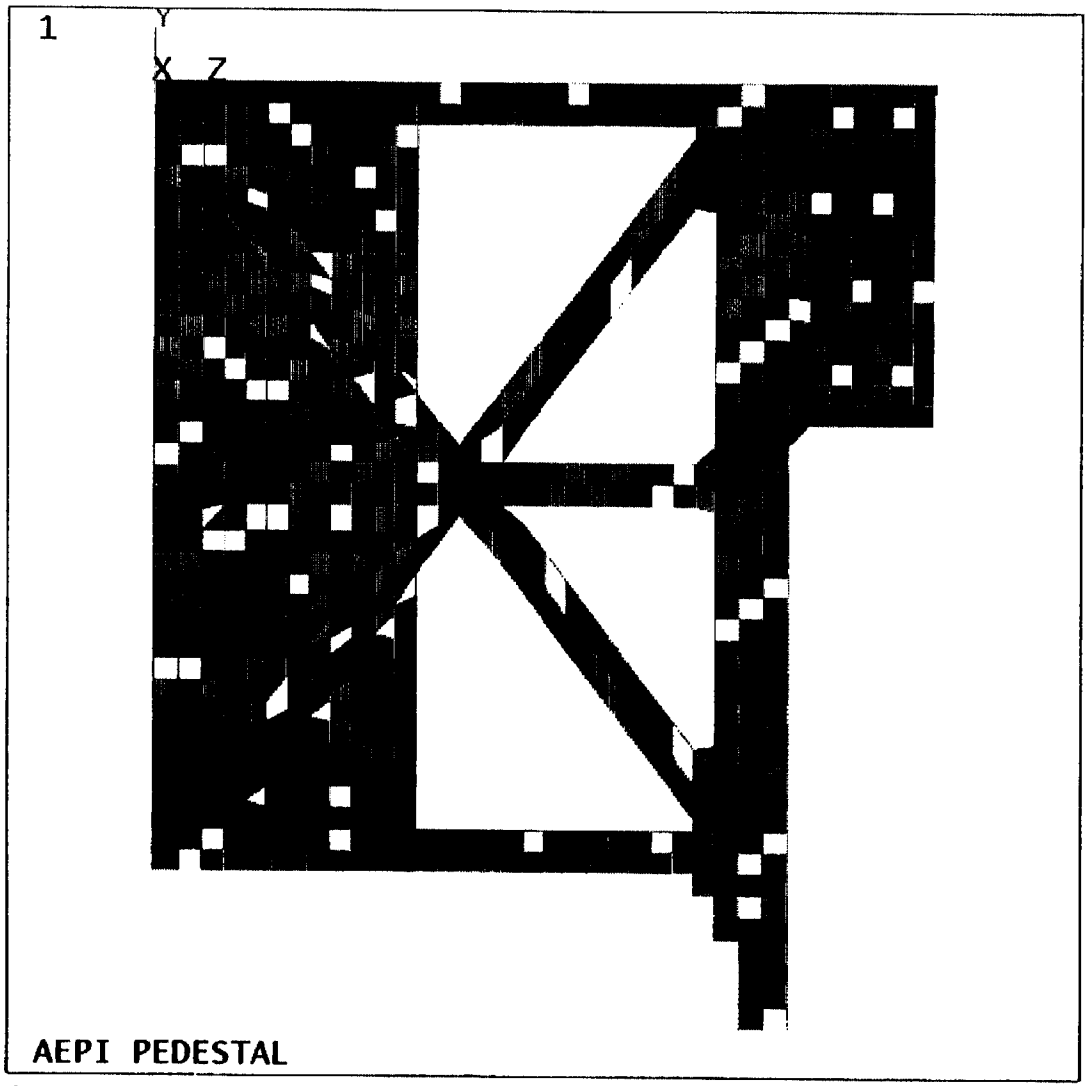

Figure 13. Pedestal model – side X = 0.0.

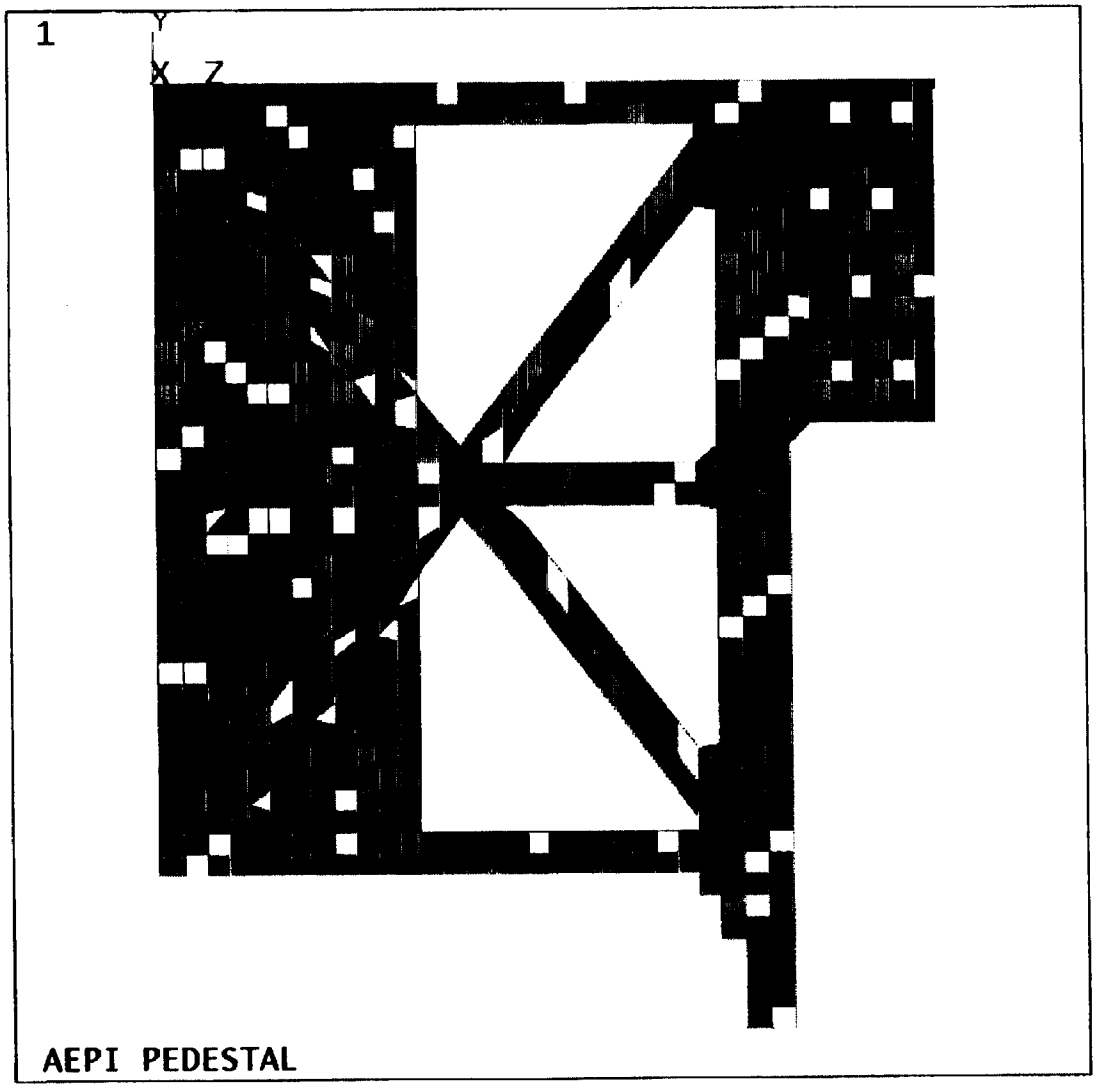

*

* SIDE PANEL (X=14.42)

*

Figure 14. Pedestal model – side X = 14.42.

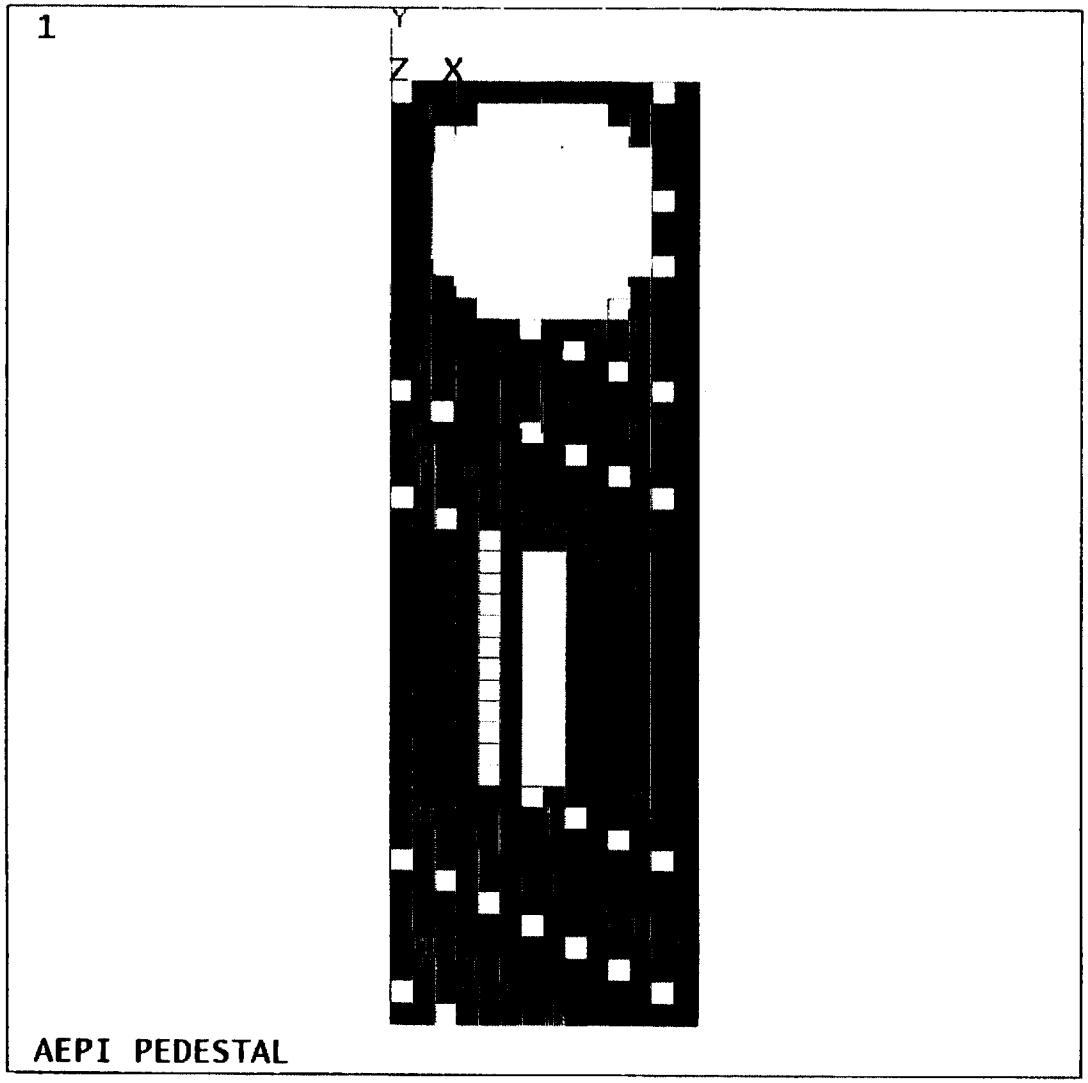

Figure 15. Pedestal model – top.

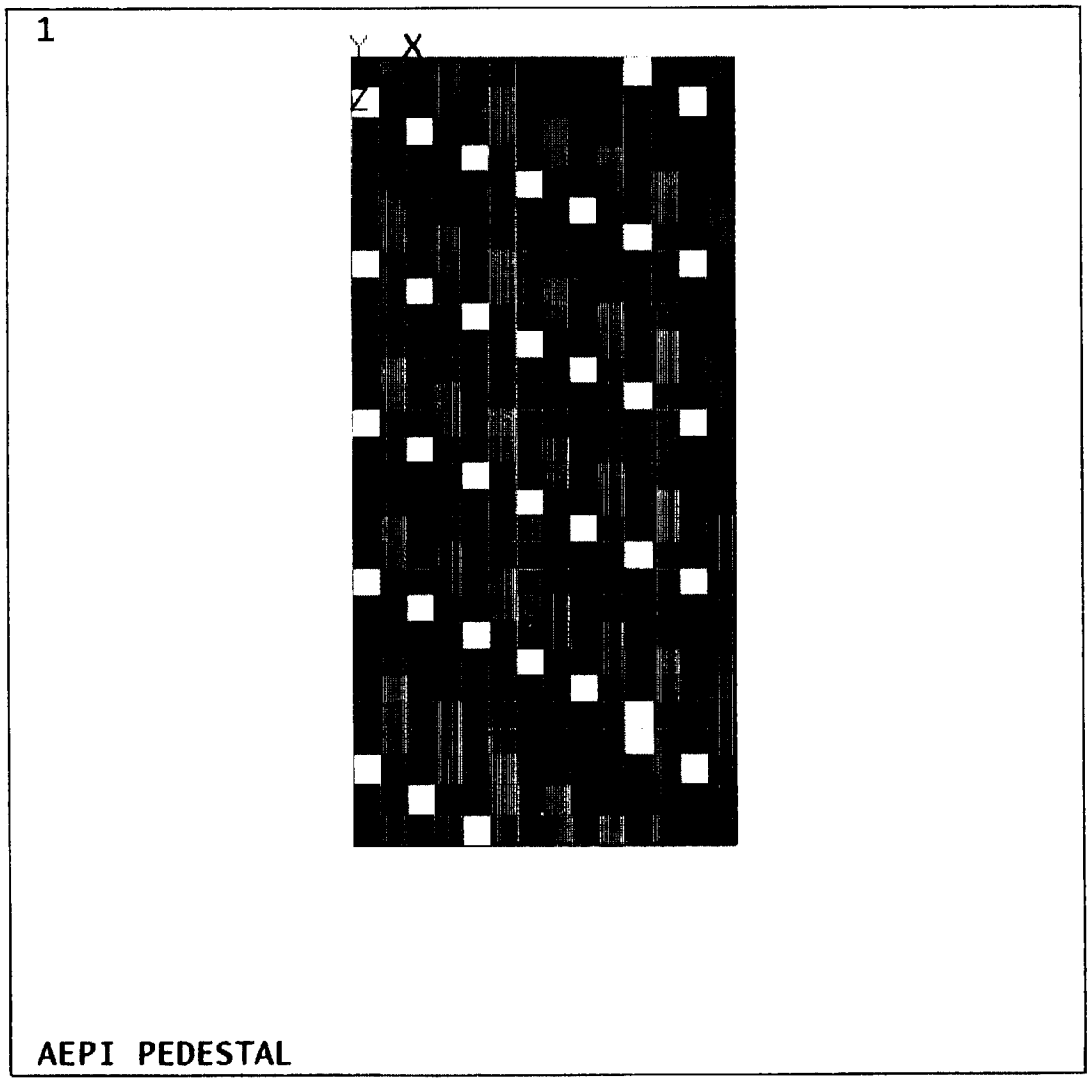

*

* SHORTER SHEAR PANEL

*

Figure 16. Pedestal model – shear panel, short.

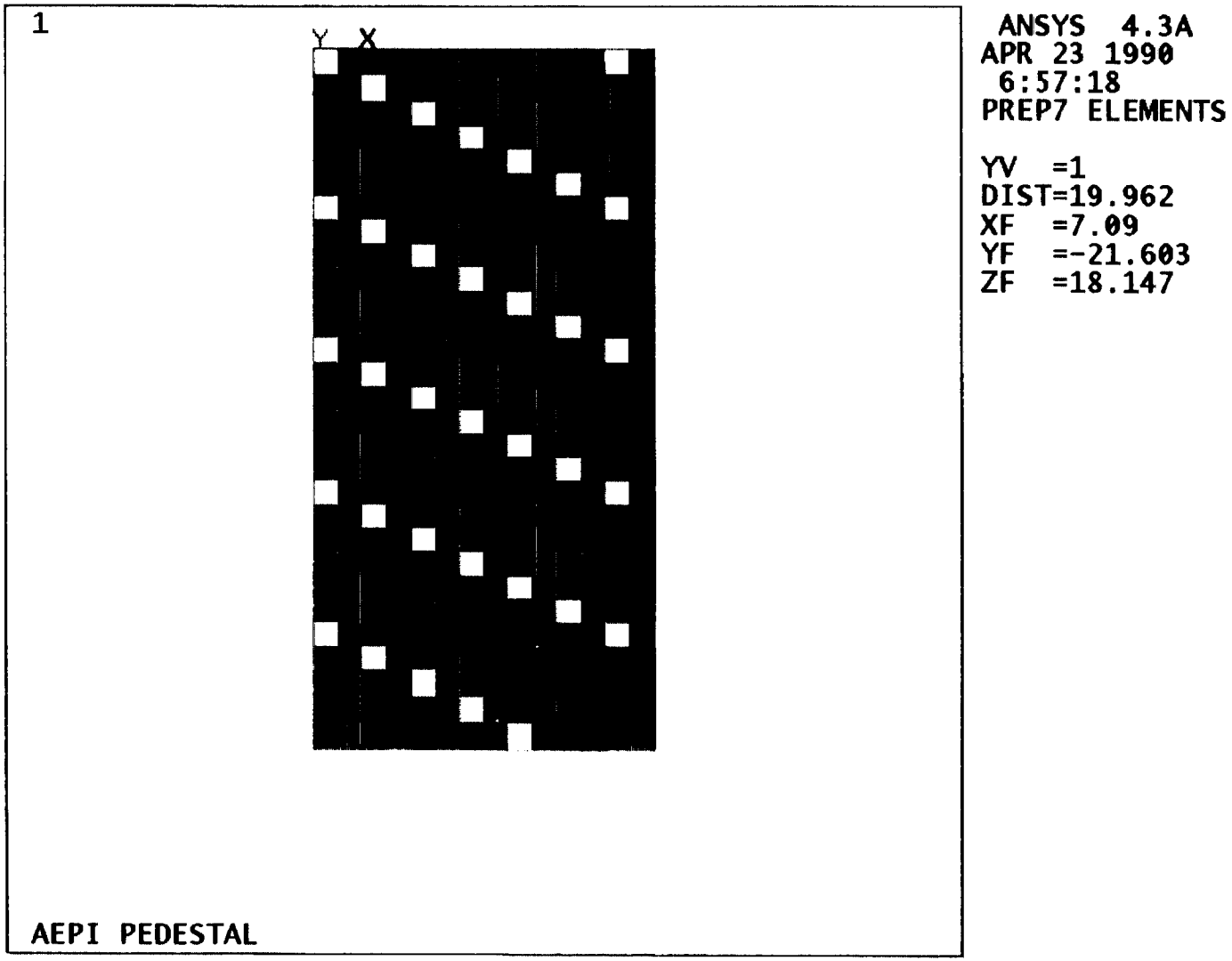

Figure 17. Pedestal model – shear panel, center.

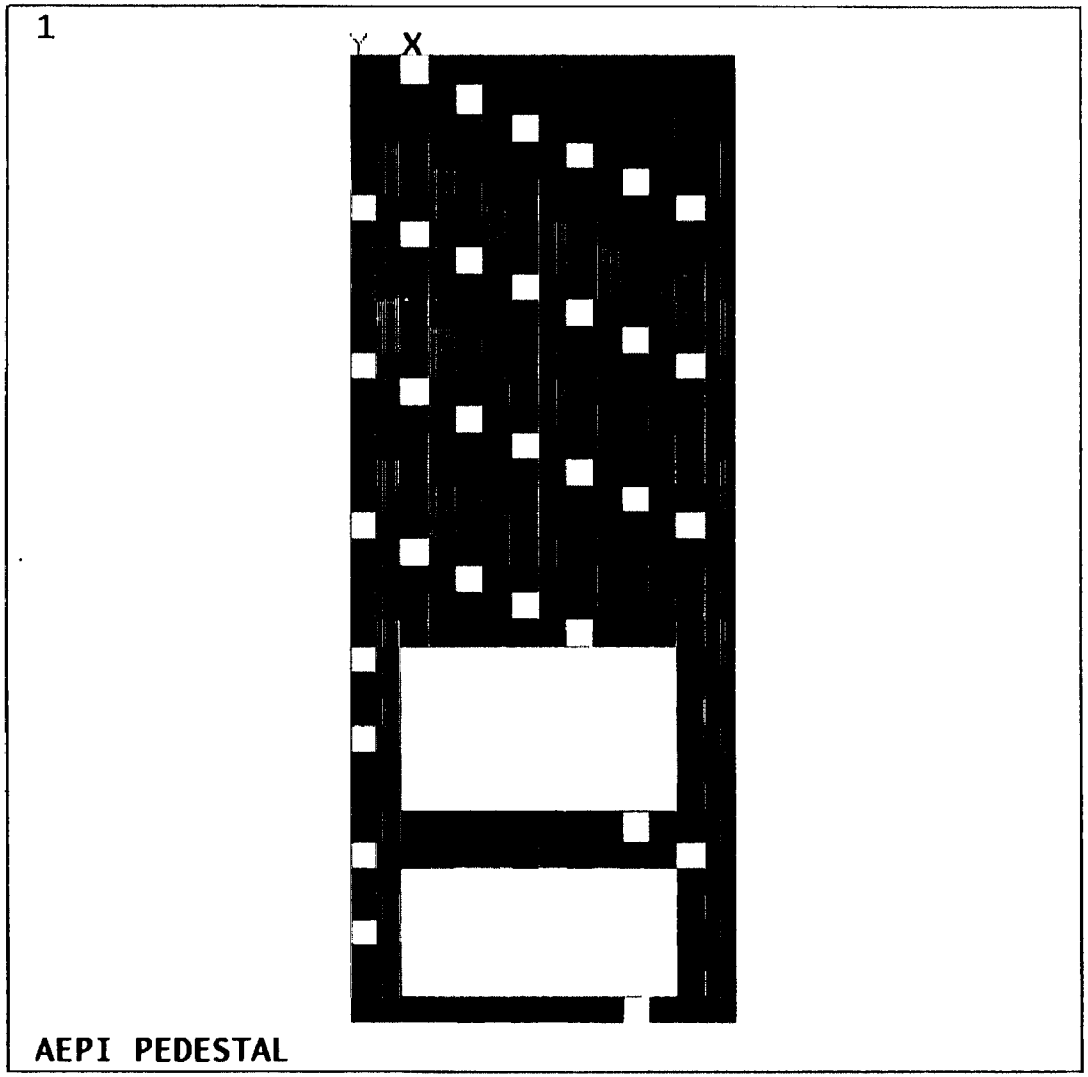

Figure 18. Pedestal model – shear panel, tall.

CASE 2

LOCATION	TEST	MODEL	%DIFFERENCE
D1	-.331	-.33007	.3%
D2	-.331	-.31963	4%
D3 *	-.319	-.26622	20%
D4	-.290	-.26607	9%
D5	.025	.01374	---
D6	.014	.01190	---
D7	.027	.01767	---
D8	.018	.00945	---
D9	-.294	-.28048	5%

CASE 6

LOCATION	TEST	MODEL	%DIFFERENCE
D1	.306	.31454	3%
D2	.308	.30443	2%
D3 *	.302	.25272	20%
D4	.268	.25306	6%
D5	-.033	-.00831	---
D6	-.010	-.00831	---
D7	-.018	-.00887	---
D8	-.014	-.01264	---
D9	.263	.26926	3%

*GAUGE SUSPECT

Figure 19. Test versus model deflections – cases 2 and 6.

CASE 3

LOCATION	TEST	MODEL	%DIFFERENCE
D1	-.335	-.32274	4%
D2	-.331	-.31013	7%
D3 *	-.319	-.26078	23%
D4	-.289	-.26019	12%
D5	.022	.01631	---
D6	.013	.01211	---
D7	.024	.01666	---
D8	.017	.01034	---
D9	-.289	-.26801	8%

CASE 7

LOCATION	TEST	MODEL	%DIFFERENCE
D1	.326	.32770	.6%
D2	.313	.31464	.6%
D3 *	.315	.26504	19%
D4	.281	.26411	7%
D5	-.026	-.01076	---
D6	-.010	-.00894	---
D7	-.015	-.01079	---
D8	-.016	-.00652	---
D9	.277	.27111	3%

*GAUGE SUSPECT

Figure 20. Test versus model deflections – cases 3 and 7.

CASE 4

LOCATION	TEST	MODEL	%DIFFERENCE
D1	-.340	-.31946	7%
D2	-.331	-.30003	11%
D3 *	-.325	-.25624	27%
D4	-.291	-.25397	15%
D5	-.005	-.03105	---
D6	-.006	-.00588	---
D7	-.007	-.01602	---
D8	.000	-.00949	---
D9	-.289	-.25956	12%

CASE 8

LOCATION	TEST	MODEL	%DIFFERENCE
D1	.319	.32539	2%
D2	.307	.30560	.5%
D3 *	.307	.26149	18%
D4	.271	.25870	5%
D5	.006	.03336	---
D6	.009	.00760	---
D7	.014	.01874	---
D8	.002	.01092	---
D9	.272	.26299	4%

*GAUGE SUSPECT

Figure 21. Test versus model deflections – cases 4 and 8.

CASE 5

LOCATION	TEST	MODEL	%DIFFERENCE
D1	-.335	-.32331	4%
D2	-.326	-.30147	9%
D3 *	-.320	-.26067	23%
D4	-.287	-.25757	12%
D5	-.009	-.02841	---
D6	-.008	-.00564	---
D7	-.011	-.01741	---
D8	-.001	-.00995	---
D9	-.284	-.25492	12%

CASE 9

LOCATION	TEST	MODEL	%DIFFERENCE
D1	.327	.32023	3%
D2	.317	.29713	7%
D3 *	.315	.25829	22%
D4	.264	.25370	5%
D5	.009	.02921	---
D6	.011	.00648	---
D7	.017	.01944	---
D8	.004	.00993	---
D9	.279	.24860	13%

*GAUGE SUSPECT

Figure 22. Test versus model deflections – cases 5 and 9.

invariants (appendix C), the invariants were plotted versus the location around the base of the pedestal (figs. 23 through 26). Please note that load case 1 was the rerun of the 1981 Spacelab 1 load.

From the data presented, the model can be considered test verified. The deflections were within 6 percent of each other, and the stress invariant plots showed their magnitude and phasing to be extremely similar. The model did tend to envelop the test cases. Where gauges were in a predominant compressive area, the magnitude was generally lower than when in tension. This effect was attributed to two causes: (1) motion of the attach base was largest on the tension side, and (2) the base attach angle reacts compressive loads with less moment than the tensile loads. The model did utilize the base motion (seen in test) as an input, but did not attempt to handle the base attach angle load path differently for compression and tension [4].

CONCLUSIONS

This report has documented the load testing (performed by the MSFC Structural Test Division) and finite element modeling accomplished on the AEPI fiberglass pedestal, which is to be launched on the space shuttle as part of the ATLAS-1 mission. Comparisons between the pedestal static loads testing results gathered for Spacelab 1 in 1981 and again in 1989 indicate that no clearly detectable stiffness changes have occurred with time, and that rosette strain gauge readings around the highly stressed pedestal base show good agreement.

Correlation of the model and test results was accomplished by comparing both the deflections and the stress invariants for eight liftoff flight load cases. The measured deflections were within 6 percent of test data, and the magnitude and phasing of the stress invariants clearly showed correlation. The model is considered test verified and is an acceptable tool for determining the margins of safety on the pedestal for flight on the ATLAS-1 mission.

Table 8 depicts the critical margins of safety calculated from the pedestal model utilizing the ATLAS-1 flight loads. As noted, the Tsai-Wu failure criteria was used for the evaluation of the fiberglass panels. The lowest margin of safety was +0.30, which represents the bearing capability of the fiberglass panel while loaded by an attach bolt [5].

In summary, the pedestal was inspected and photographed in visible and ultraviolet light before and after being statically tested to 120 percent X ATLAS-1 flight loads. No detectable changes in the hardware were discovered; thus, the AEPI fiberglass pedestal is considered structurally certified for flight.

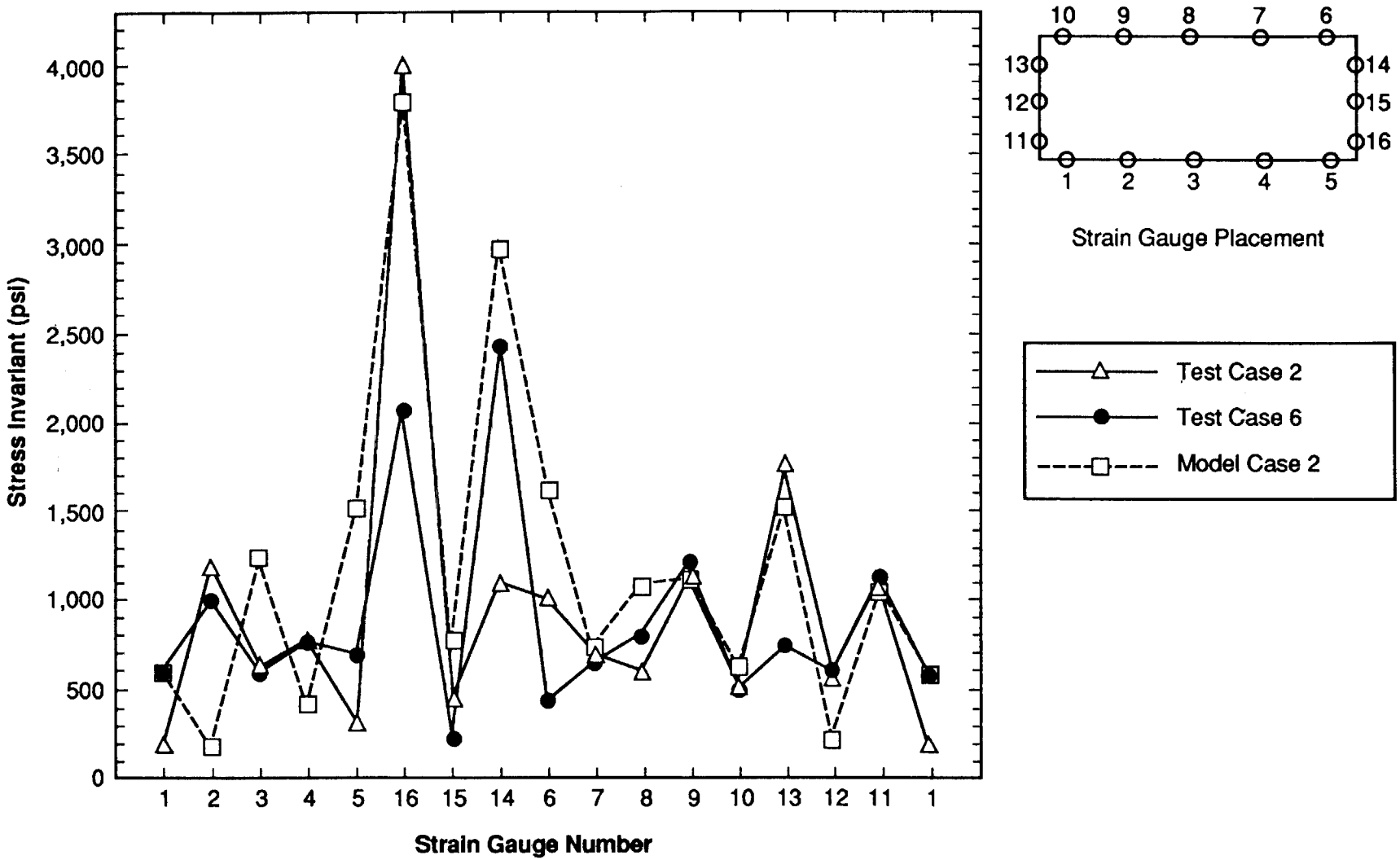

Figure 23. Comparison of stress invariants for the model and test – cases 2 and 6.

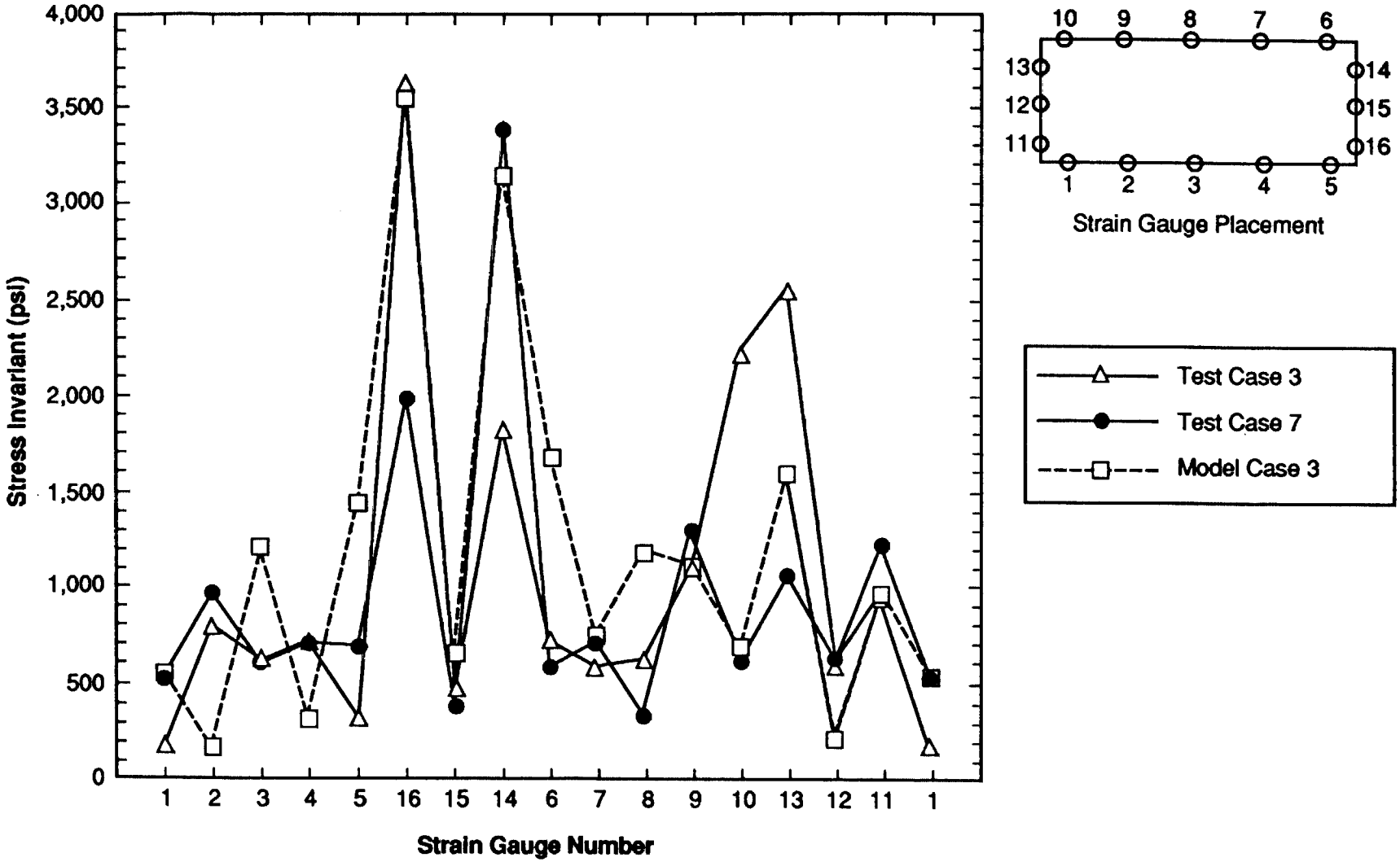

Figure 24. Comparison of stress invariants for the model and test – cases 3 and 7.

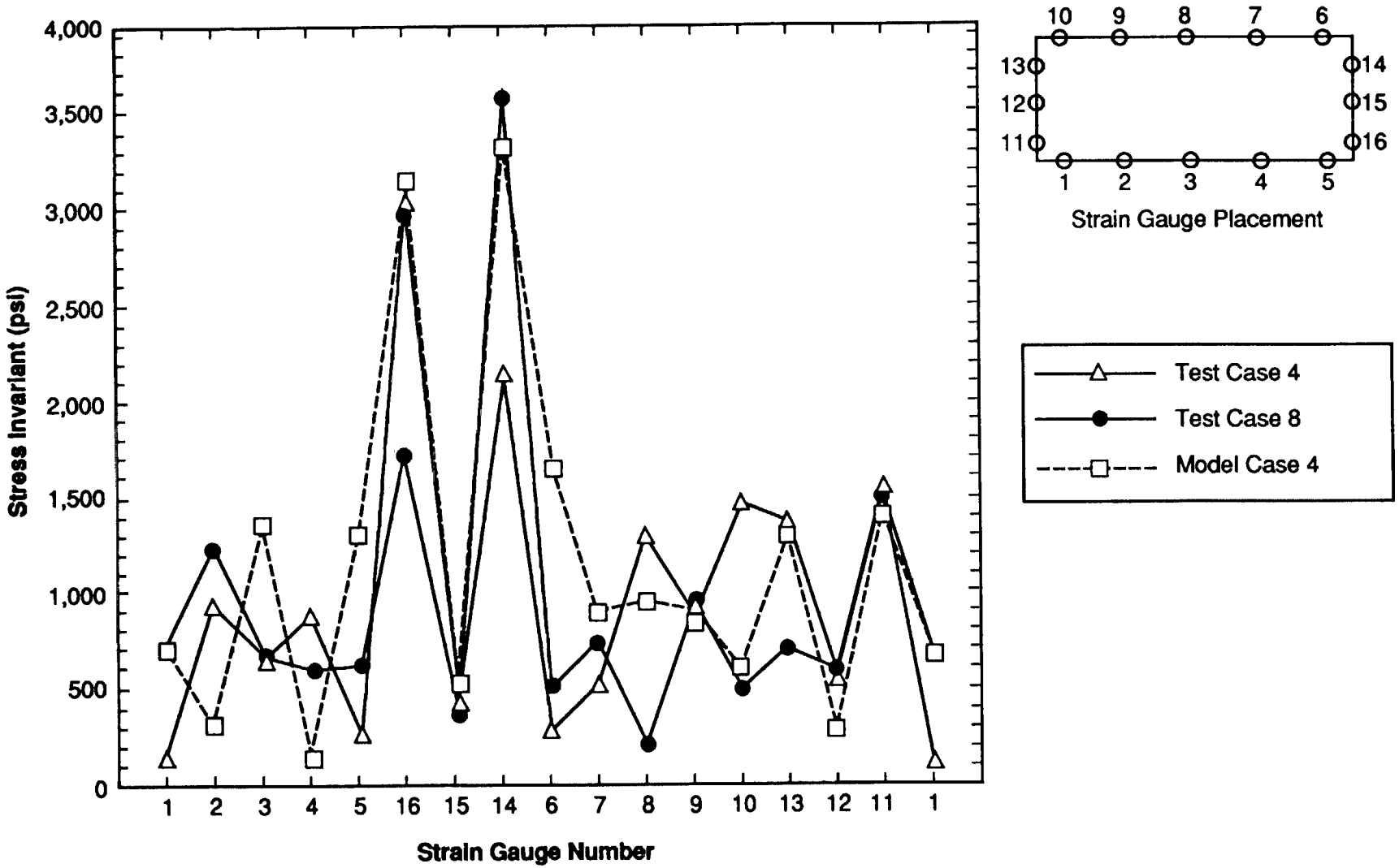

Figure 25. Comparison of stress invariants for the model and test – cases 4 and 8.

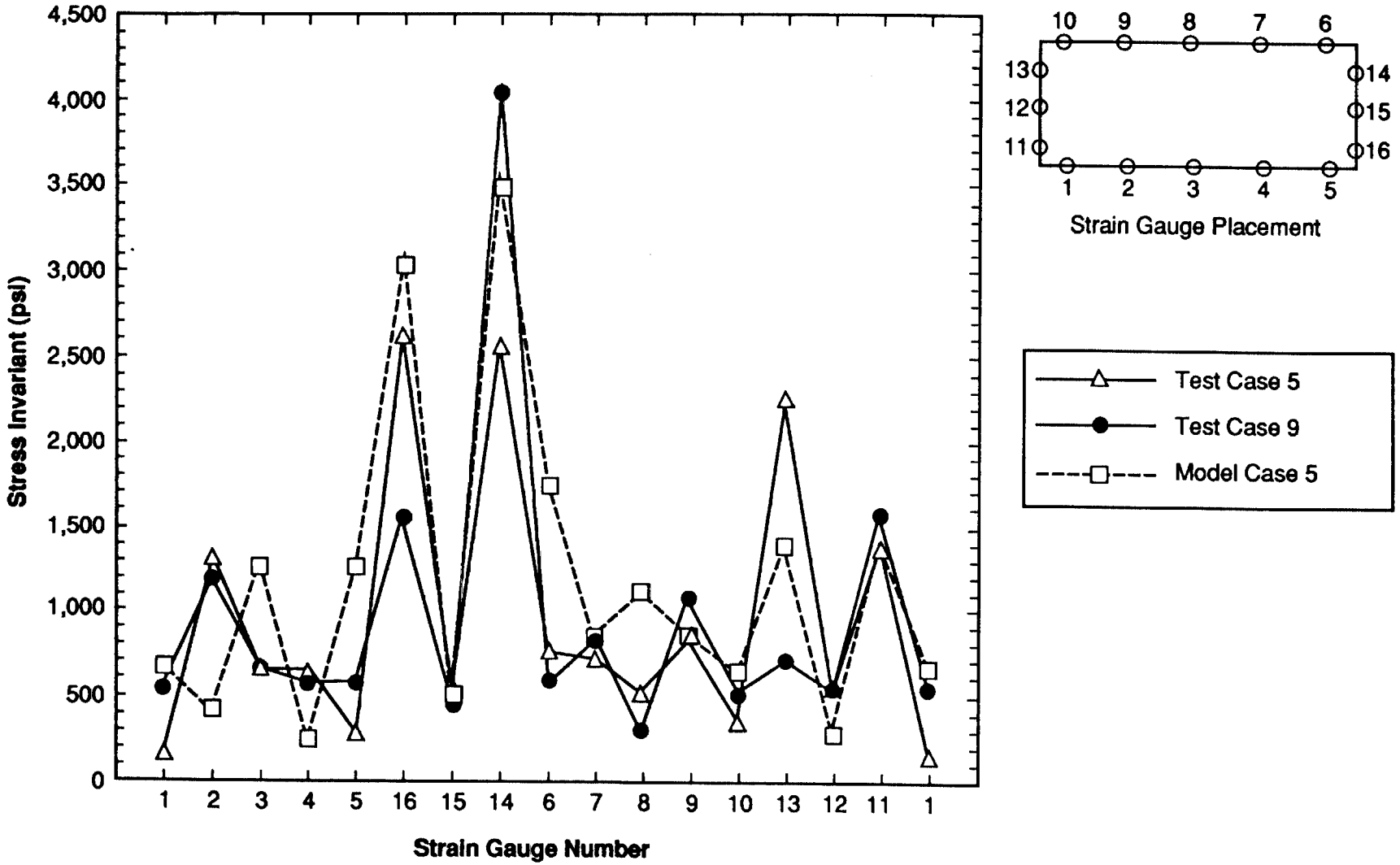

Figure 26. Comparison of stress invariants for the model and test – cases 5 and 9.

Table 8. Margin of safety summary for AEPI pedestal model.

Item	Material	Strength	Load	M.S.	Remarks
Base Angle	2219-T87	47 ksi yield 63 ksi ult.	4.3 ksi 4.3 ksi	+9 +9	
Taller Shear Panel	Fiberglass	1	.0272	+17	Tsai-Wu failure*
Center Shear Panel	Fiberglass	1	.01895	+25	Tsai-Wu failure*
Shorter Shear Panel	Fiberglass	1	.01363	+36	Tsai-Wu failure*
Top	Fiberglass	1	.04988	+9	Tsai-Wu failure*
Sides	Fiberglass	1	.07602	+5	Tsai-Wu failure*
Lens Cover/ Pedestal Attachment	Fiberglass	8600 psi	265 psi	+22	Bearing
Gimbal Attachment	Fiberglass	14560 psi	2583 psi	+3	Bearing
Cradle Brackets Attachment	Fiberglass	14440 psi	7659 psi	+.3	Bearing
Electronics Box Attachment	Fiberglass	11660 psi	1250 psi	+5	Bearing
Base Angle Bolts	A-286	4438 lbs. 2695 lbs.	2506 lbs 591 lbs	+.69	Tension Shear
All Fiberglass Structure	Fiberglass	2100 psi	437 psi	+1.4**	Interlam. Shear

* $A_{11}\sigma_x^2 + 2A_{12}\sigma_x\sigma_y + A_{22}\sigma_y^2 + A_{66}\tau_{xy}^2 + B_1\sigma_x + B_2\sigma_y = 1$

** F.S. of 2.0 was used since allowable is from vendor data.

REFERENCES

1. MSFC letter EJ21 (54-90), Recertification of AEPI Fiberglass Pedestal for the ATLAS-1 Mission, May 5, 1990.

2. MSFC letter ED25 (90-48), Summary of AEPI Fiberglass Pedestal Structural Loads Testing for the ATLAS-1 Mission, March 14, 1990.

3. MSFC letter ED25 (90-2), Transmittal of Structural Test Requirements Document for the AEPI Fiberglass Pedestal, January 9, 1990.

4. MSFC letter ED25 (90-65), Summary of AEPI Fiberglass Pedestal Test Verification of Finite Element Model, March 30, 1990.

5. MSFC letter ED25 (90-66), Summary of AEPI Fiberglass Pedestal Margins of Safety From the Finite Element Model, March 27, 1990.

6. EDSU International Ltd. Structures Manual, Composites Volume 5, Item Number 83014, pages 8–12.

APPENDIX A

DEPLY ANALYSIS OF AEPI FIBERGLASS

Three dogbone specimens from the group cut out of the scrap dome section were thermally deplied and fiber angles carefully measured. An analysis of predicted strength, based on previously obtained data from 1981 giving ultimate strengths for various pull directions with respect to the bidirectional cloth, was performed using the software package titled "Utah Laminates." This program gives values for material moduli, but past experience has shown that altering the modulus of a material by changing the layup configuration will give approximately the same percentage change in strength. Actually, the strength will decrease slightly more than the modulus when a unidirectional composite is changed to a quasi-isotropic configuration which approximates the case being investigated. Since the actual material consists of laminae of woven cloth with a strong and weak direction, it is assumed that as an average half the measurements were in the strong direction and half were in the weak direction. This was accounted for in the program. The results are given below:

Specimen No.	1	2	3
Fiber Angle	80	–50	60
	–10	60	–60
	70	–40	40
	–30	45	–55
	80	–45	30
	–30	70	–20
	80	–30	5
	–35	40	–50
	60	–55	15
	–40	50	–35
	55	–5	75
	–25	70	–10
	60	–35	60
	–35	70	–20
	55	–10	80
	–10	70	–10
	70		
	17 plies total	16 plies total	16 plies total
Theoretical Breaking Stress:	30,000 psi	28,900 psi	33,200 psi

Tests done by MSFC in June 1989.
Samples were cut from spare bumper rail dome – random layup.

Data for F-161/1581 (Fiberglass) Material

Tensile Load to Failure

Crosshead Rate = 0.10 in/min

Temperature = 77 °F

Humidity = 70%

Average Breaking Strength = 31,721 psi

Standard Deviation = 1,990 psi

F-161/1581 Thursday, June 22, 1989, 1:50 p.m.

Specimen No.	Width (in)	Thickness (in)	Load (lb)	Strength (psi)
1 1.000	0.500	0.196	2,810.000	28,673.000
2 2.000	0.495	0.194	3,070.000	31,969.000
3 3.000	0.495	0.195	2,900.000	30,044.000
4 4.000	0.500	0.195	3,305.000	33,897.000
5 5.000	0.505	0.198	3,250.000	32,503.000
6 6.000	0.504	0.197	3,300.000	33,237.000

APPENDIX B

CALCULATION OF 1981 TEST STRAINS

The AEPI testing accomplished in 1981 took the triaxial strain gauge readings directly from the test and input them into a computer program which generated principal stresses (σ_{max}, σ_{min}, τ_{max}, and θ). These data were generated by using an isotropic Mohr's circle approach. In order to compare the strains derived from the 1981 and 1989 tests, the 1981 strain components must be derived.

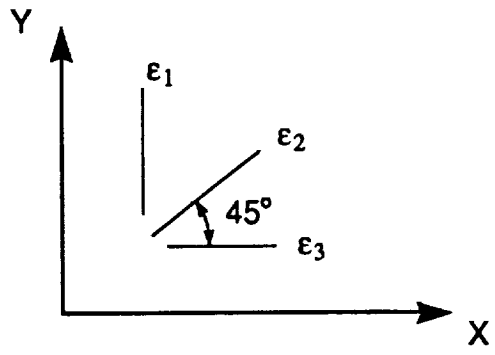

The following defines how that was accomplished:

– The basic Mohr's circle is shown below.

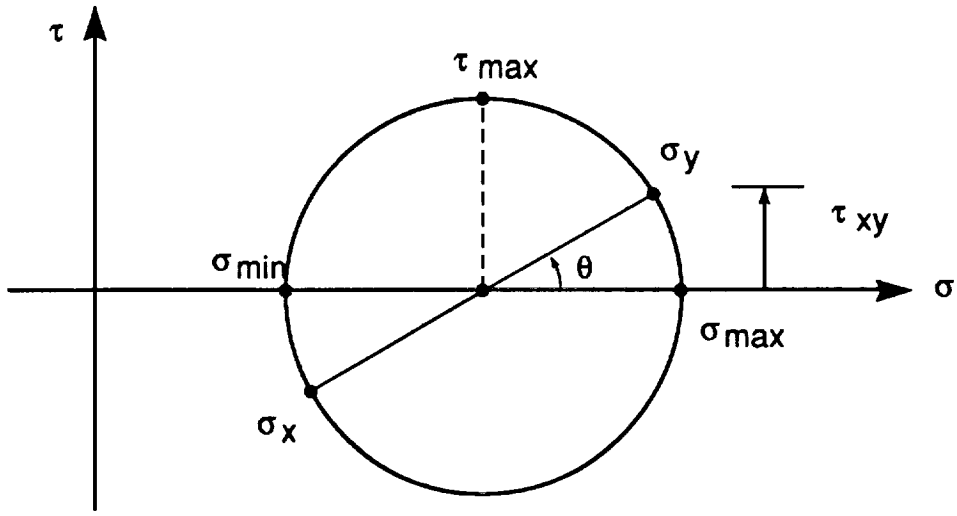

$$\cos\theta = \frac{\sigma_y - \left(\frac{\sigma_{max} + \sigma_{min}}{2}\right)}{\tau_{max}}$$

– From this equation σ_y can be calculated

$$\sigma_y = \tau_{max} \cos\theta + \frac{\sigma_{max} + \sigma_{min}}{2}$$

– Knowing that $\sigma_{max} + \sigma_{min} = \sigma_x + \sigma_y$

$$\sigma_x = \sigma_{max} + \sigma_{min} - \sigma_y$$

– Since: $\sin\theta = \tau_{xy}/\tau_{max}$

$$\tau_{xy} = \tau_{max} \sin\theta$$

The stress-strain matrix equation is

$$\begin{Bmatrix} \varepsilon_x \\ \varepsilon_y \\ \frac{\gamma_{xy}}{2} \end{Bmatrix} = \begin{bmatrix} 1/E & -\nu/E & 0 \\ -\nu/E & 1/E & 0 \\ 0 & 0 & 1/G \end{bmatrix} \begin{Bmatrix} \sigma_x \\ \sigma_y \\ \tau_{xy} \end{Bmatrix}$$

So

$$\boxed{\varepsilon_x = \frac{\sigma_x}{E} - \frac{\nu\sigma_y}{E} \equiv \varepsilon_3}$$

$$\boxed{\varepsilon_y = \frac{-\nu\sigma_x}{E} + \frac{\sigma_y}{E} \equiv \varepsilon_1}$$

$$\frac{\gamma_{xy}}{2} = \frac{\tau_{xy}}{G} \qquad \text{and} \qquad \frac{\gamma_{xy}}{2} = \frac{\varepsilon_1 + \varepsilon_3}{2} - \varepsilon_2$$

hence

$$\varepsilon_2 = \frac{\varepsilon_1 + \varepsilon_3}{2} - \frac{\gamma_{xy}}{2}$$

These component strains (ε_1,ε_2,ε_3) were then directly compared with the 1989 test triaxial strains.

APPENDIX C

STRESS INVARIANT CALCULATIONS

The stress invariant used in this analysis is:

$$\sigma_{inv} = (\sigma_x^2 - \sigma_x\sigma_y + \sigma_y^2 + 3\tau_{xy}^2)^{1/2}$$

where:

σ_x = tensile or compression stress in x-axis

σ_y = tensile or compression stress in y-axis

τ_{xy} = shear stress in x-y plane

The test data comes from triaxial strain gauges.

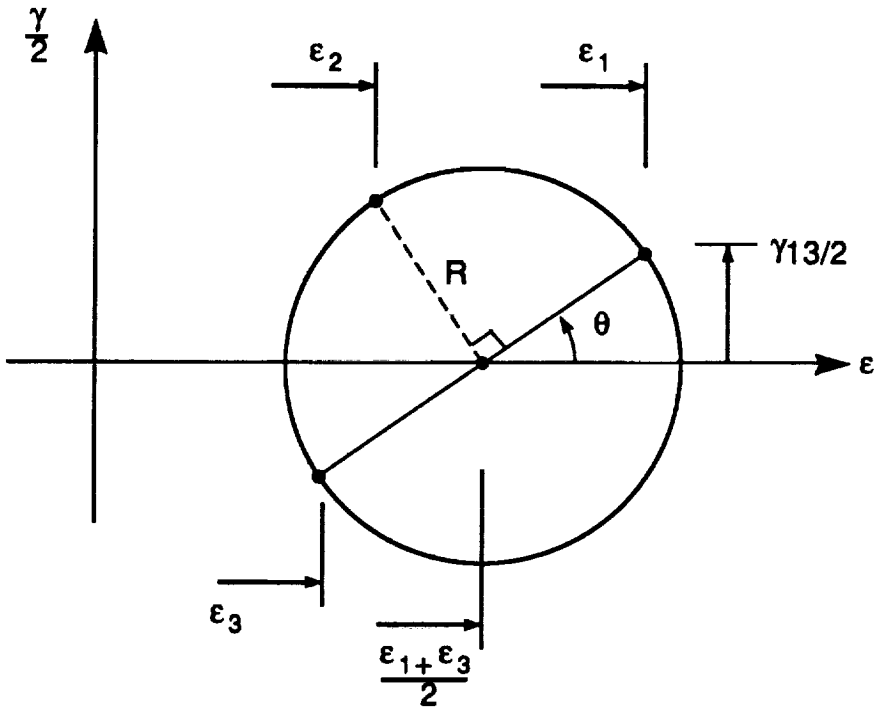

$$\sin\theta = \frac{\gamma_{13/2}}{R}$$

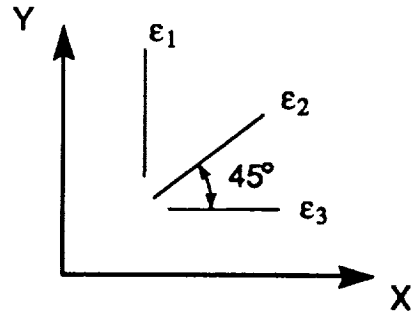

and

$$\sin\theta = \frac{\frac{\varepsilon_1+\varepsilon_3}{2} - \varepsilon_2}{R}$$

so that

$$\gamma_{13/2} = \frac{\varepsilon_1+\varepsilon_3}{2} - \varepsilon_2$$

Material properties used:

$$E_x = 2.9\times10^6 \text{ psi}$$

$$E_y = 3.0\times10^6 \text{ psi}$$

$$G_{xy} = 0.45\times10^6 \text{ psi}$$

$$\nu = 0.12.$$

I. For plane stress panels (0, 90° layup)

$$\begin{Bmatrix} \sigma_x \\ \sigma_y \\ \tau_{xy} \end{Bmatrix} = \begin{bmatrix} C_{xx} & C_{xy} & 0 \\ C_{yx} & C_{yy} & 0 \\ 0 & 0 & C_{zz} \end{bmatrix} \begin{Bmatrix} \varepsilon_x \\ \varepsilon_y \\ \gamma_{xy}/2 \end{Bmatrix}$$

where

$$C_{xx} = \frac{E_x}{1-\nu^2} \qquad C_{yy} = \frac{E_y}{1-\nu^2}$$

$$C_{xy} = \frac{\nu E_y}{1-\nu^2} \qquad C_{yx} = \frac{\nu E_x}{1-\nu^2} \qquad C_{zz} = G_{xy}$$

From this

$$\sigma_x = 2.9423\ \varepsilon_x + 0.3652\ \varepsilon_y$$

$$\sigma_y = 0.3530\ \varepsilon_x + 3.0438\ \varepsilon_y$$

$$\tau_{xy} = 0.45\ \gamma_{xy}/2$$

and translating into test nomenclature:

$$\sigma_x = 2.9423\ \varepsilon_3 + 0.3652\ \varepsilon_1$$

$$\sigma_y = 0.3530\ \varepsilon_3 + 3.0438\ \varepsilon_1$$

$$\tau_{xy} = 0.45\ [(\varepsilon_1 + \varepsilon_3)/2 - \varepsilon_2]$$

panels with 0, 90° layup.

The invariant magnitude can then be calculated.

II. For plane stress panels (±45° layup)

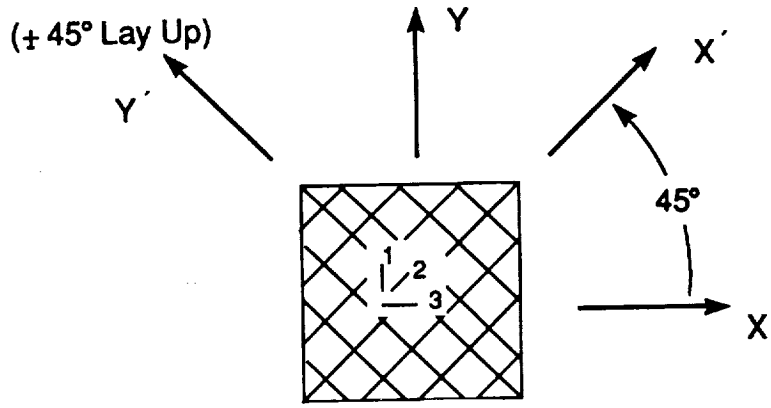

– From matrix transformation equation

$$\{\varepsilon\} = [J^T]\{\varepsilon'\}$$

where

$$[J^T] = \begin{bmatrix} 0.5 & 0.5 & -0.5 \\ 0.5 & 0.5 & 0.5 \\ 1.0 & -1.0 & 0 \end{bmatrix}$$

so

$$\begin{Bmatrix} \varepsilon_x \\ \varepsilon_y \\ \gamma_{xy}/2 \end{Bmatrix} = [J^T] \begin{Bmatrix} \varepsilon_x' \\ \varepsilon_y' \\ \gamma_{x'y'}/2 \end{Bmatrix} \quad ; \qquad \varepsilon_{x'} = \varepsilon_2$$

from Mohr's circle

$$\sin \theta = \frac{\gamma_{x'y'}/2}{R}$$

and

$$sin\ \theta = \frac{\dfrac{\varepsilon_1 + \varepsilon_3}{2} - \varepsilon_1}{R}$$

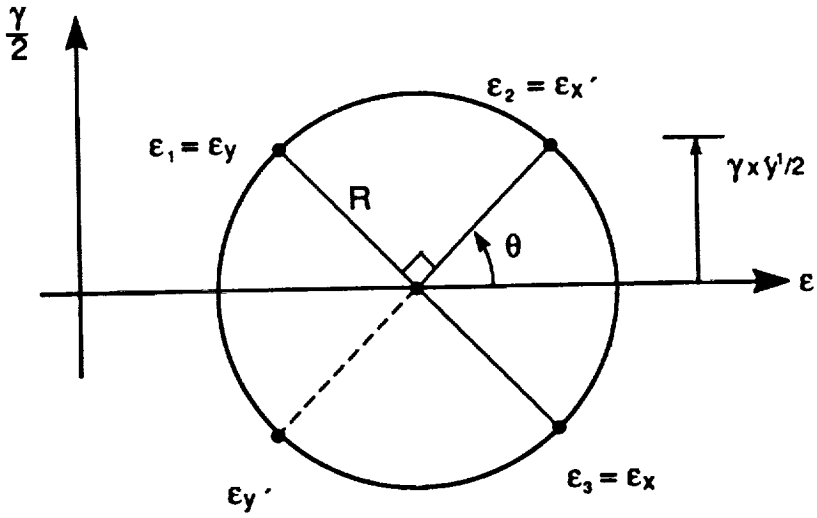

so

$$\frac{\gamma_{x'y'}}{2} = \frac{\varepsilon_3 - \varepsilon_1}{2}$$

and knowing that

$$\varepsilon_1 + \varepsilon_3 = \varepsilon_2 + \varepsilon_{y'}$$

$$\varepsilon_{y'} = \varepsilon_1 - \varepsilon_2 + \varepsilon_3$$

using the transformation matrix

$$\{\varepsilon\} = [J^T] \{\varepsilon'\}$$

and the stress-strain matrix

$$\{\sigma'\} = [C'] \{\varepsilon'\}$$

where

$$C_{x'x'} = \frac{E_{x'}}{1-\nu^2}$$

$$C_{y'y'} = \frac{E_{y'}}{1-\nu^2}$$

$$C_{x'y'} = \frac{\nu E_{y'}}{1-\nu^2}$$

$$C_{y'x'} = \frac{\nu E_{x'}}{1-\nu^2}$$

$$C_{z'z'} = G_{x'y'}$$

Material properties used

$$E_{x'} = 2.9 \times 10^6 \text{ psi}$$

$$E_{y'} = 3.0 \times 10^6 \text{ psi}$$

$$G_{x'y'} = 0.45 \times 10^6 \text{ psi}$$

$$\nu = 0.12$$

using the transformation matrix

$$\{\sigma\} = [J]^{-1} \{\sigma'\}$$

where

$$[J]^{-1} = \begin{bmatrix} 0.5 & 0.5 & -1.0 \\ 0.5 & 0.5 & 1.0 \\ 0.5 & -0.5 & 0 \end{bmatrix}$$

so that

$$\{\sigma\} = [J]^{-1} [C'] \{\varepsilon'\}$$

performing proper substitution

$$\{\sigma\} = [J]^{-1}\,[C']\begin{Bmatrix} \varepsilon_2 \\ \varepsilon_1 - \varepsilon_2 + \varepsilon_3 \\ \dfrac{\varepsilon_3 - \varepsilon_1}{2} \end{Bmatrix}$$

translating into test nomenclature:

$$\sigma_x = 1.9295\ \varepsilon_1 - 0.0569\ \varepsilon_2 + 1.4795\ \varepsilon_3$$

$$\sigma_y = 1.4795\ \varepsilon_1 - 0.0569\ \varepsilon_2 + 1.9295\ \varepsilon_3$$

$$\tau_{xy} = -1.3393\ \varepsilon_1 + 2.6339\ \varepsilon_2 - 1.3393\ \varepsilon_3$$

The invariant magnitude can then be calculated.

APPENDIX D

MATERIAL PROPERTY CALCULATIONS

This appendix will show how calculations were made for (I) the ultimate shear strength (Fsu) for the fiberglass panels, and (II) the Tsai-Wu criterion coefficients.

(I). Calculation of Fsu for fiberglass panels.

The fiberglass panels were tested to σ_x' stress level. Thus

$$\{\sigma\} = [J]\{\sigma'\}$$

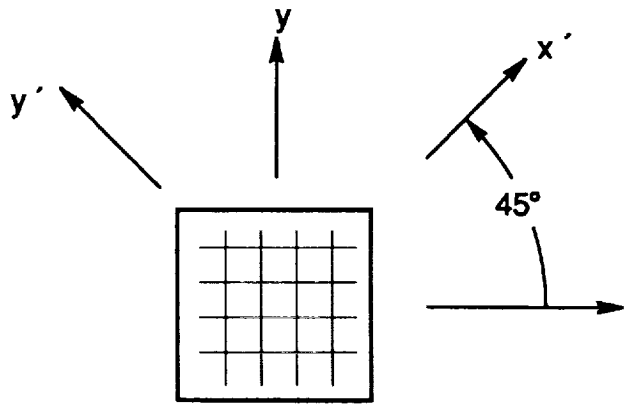

where

$$[J] = \begin{bmatrix} 0.5 & 0.5 & 1.0 \\ 0.5 & 0.5 & -1.0 \\ -0.5 & 0.5 & 0.0 \end{bmatrix}$$

hence

$$\begin{Bmatrix} \sigma_x \\ \sigma_y \\ \tau_{xy} \end{Bmatrix} = \begin{bmatrix} 0.5 & 0.5 & 1.0 \\ 0.5 & 0.5 & -1.0 \\ -0.5 & 0.5 & 0.0 \end{bmatrix} \begin{Bmatrix} \sigma_x' \\ \sigma_y' \\ \tau_{x'y'} \end{Bmatrix}$$

from this simple matrix:

$$\tau_{xy} = -0.5\sigma_x' + 0.5\sigma_y'$$

if $\sigma_y' = 0$, then

$$\boxed{\tau_{xy} = \frac{\sigma_x'}{2}}$$

thus

$$Fsu = \frac{21.5 \text{ Ksi}}{2} \simeq 10.7 \text{ Ksi}$$

(II). Calculation of the Tsai-Wu Failure Criterion Coefficients

This is a general criterion applicable to anisotropic laminates in plane stress. Considering a single orthotropic layer under plane stress aligned with the principal axes of orthotropy, the general expression reduces to [6]:

$$A_{11}\sigma_x^2 + 2A_{12}\sigma_x\sigma_y + A_{22}\sigma_y^2 + A_{66}\tau_{xy}^2 + B_1\sigma_x + B_2\sigma_y = 1/\text{factor of safety}$$

By substituting allowable values of uniaxial and shear stresses into their respective places, where

$$\sigma_x = Ftu_x = Fcu_x = 43.3 \text{ Ksi}$$

$$\sigma_y = Ftu_y = Fcu_y = 36.2 \text{ Ksi}$$

$$\tau_{xy} = Fsu = 10.7 \text{ Ksi}$$

then the coefficients can be expressed as:

$$A_{11} = \frac{1}{(Ftu_x)(Fcu_x)} = 5.3336 \times 10^{-4}$$

$$A_{22} = \frac{1}{(Ftu_y)(Fcu_y)} = 7.6310 \times 10^{-4}$$

$$A_{66} = \frac{1}{(\text{Fsu})^2} = 8.7343 \times 10^{-3}$$

$$B_1 = \frac{1}{(\text{Ftu}_x)} - \frac{1}{(\text{Fcu}_x)} = 0.0$$

$$B_2 = \frac{1}{(\text{Ftu}_y)} - \frac{1}{(\text{Fcu}_y)} = 0.0$$

The remaining term, A_{12}, must come from a biaxial test, which was accomplished as shown in the sketch below:

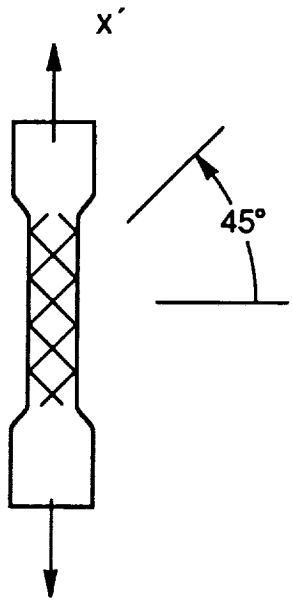

This term can now be expressed as a function of the unidirectional allowable stresses and an additional stress σ_x' which must be determined by the test.

The equation using such a 45° off-axis tension test in which

$$\frac{\sigma_x'}{2} = \sigma_x = \sigma_y = \tau_{xy}$$

is:

$$A_{12} = \frac{2}{\sigma_x'^2}\left[1 - \frac{\sigma_x'}{2}\left(\frac{1}{\text{Ftu}_x} - \frac{1}{\text{Fcu}_x} + \frac{1}{\text{Ftu}_y} - \frac{1}{\text{Fcu}_y}\right) - \frac{\sigma_x'^2}{4}\left(\frac{1}{(\text{Ftu}_x)(\text{Fcu}_x)} + \frac{1}{(\text{Ftu}_y)(\text{Fcu}_y)} + \frac{1}{\text{Fsu}^2}\right)\right]$$

where σ_x' is the applied direct tensile stress during the test (21.5 Ksi). Hence

$$A_{12} = 6.8876 \times 10^{-4}$$

With all the coefficients now established, stresses in Ksi can be input, and the resulting margin of safety calculated:

$$\text{M.S.} = \frac{1}{(\text{Factor of Safety})(\text{Tsai-Wu Value})} - 1$$

APPROVAL

TEST AND MODEL CORRELATION OF THE ATMOSPHERIC EMISSION PHOTOMETRIC IMAGER FIBERGLASS PEDESTAL

By H.M. Lee III and L.A. Barker

The information in this report has been reviewed for technical content. Review of any information concerning Department of Defense or nuclear energy activities or programs has been made by the MSFC Security Classification Officer. This report, in its entirety, has been determined to be unclassified.

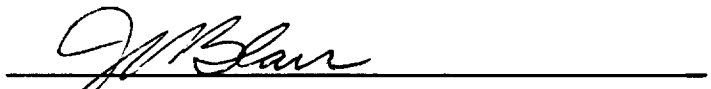

JAMES C. BLAIR
Director, Structures and Dynamics Laboratory

☆ U.S. GOVERNMENT PRINTING OFFICE 1990–531–081/20226